BRIGHAM YOUNG UNIVERSITY

GEOLOGY STUDIES

VOLUME 37 • 1991

BRIGHAM YOUNG UNIVERSITY GEOLOGY STUDIES

Volume 37, 1991

CONTENTS

A Publication of the
Department of Geology
Brigham Young University
Provo, Utah 84602

Brigham Young University Geology Studies is published by the Department of Geology. This publication consists of graduate student and faculty research within the department as well as papers submitted by outside contributors. Each article submitted by BYU faculty and outside contributors is externally reviewed by at least two qualified persons.

ISSN 0068-1016
4-91 600 48965

Carbonate Microfacies and Related Conodont Biofacies, Mississippian-Pennsylvanian Boundary Strata, Granite Mountain, West Central Utah

JARED R. MORROW
GARY D. WEBSTER
Department of Geology, Washington State University, Pullman, Washington 99164-2812

ABSTRACT

Carbonate microfacies and corresponding conodont biofacies were analyzed from four sections within the lower portion of the Ely Limestone at Granite Mountain, west central Utah. Nine recurring carbonate microfacies and two recurring conodont biofacies were recognized in these sections, each of which span the Mississippian-Pennsylvanian boundary. The microfacies present are typically thin and varied, representing a wide range of depositional fabrics and textures ranging from lime mudstones to well-sorted skeletal grainstones.

Conodont faunas present in the boundary interval are dominated by species of *Adetognathus, Cavusgnathus,* and *Rhachistognathus,* which compose nearly 96% of all conodonts recovered. Alternating dominance of conodont genera allows definite recognition of two previously proposed shallow-water biofacies: the *Adetognathus* biofacies and the *Rhachistognathus* biofacies. Elements of *Declinognathodus* and *Gnathodus* do not occur in sufficient abundance to allow recognition of other proposed Carboniferous biofacies defined by the dominance of these genera. Plots of conodont platform abundances versus carbonate Standard Microfacies (SMF) Types show that within the *Adetognathus* biofacies, the species *A. lautus* dominates over *A. spathus* in all microfacies. *Adetognathus unicornis,* although occurring stratigraphically below other *Adetognathus* species, is also less common than *A. lautus* in SMF Types that are common to both their ranges. Similarly, within the *Rhachistognathus* biofacies, *R. primus* appears more abundant than *R. muricatus, R. prolixus,* and *R. websteri* in virtually all microfacies. Greatest overall abundances of both *Adetognathus* and *Rhachistognathus* occur within the bioclast packstone and grainstone microfacies, in which an inverse occurrence pattern is seen. The microfacies and biofacies noted in the study are placed within the context of an offshore barrier shoal to nearshore lagoon depositional model for the lower Ely Limestone.

INTRODUCTION

Granite Mountain is located at the northeastern end of the Confusion Range, southern Juab County, west central Utah (fig. 1), within the eastern portion of the Basin and Range Province. At this locality, the Mississippian-Pennsylvanian boundary interval is well-exposed in the lower portion of the Ely Limestone, a shallow-water marine carbonate unit recognized over an area of 50,000 square km in western Utah and eastern Nevada (Hose 1974, Steele 1960). The presence of a diverse and locally abundant macro- and microfauna and microflora, coupled with inferred continuous deposition across the systemic boundary, has placed Granite Mountain among several western U.S. sections that are being examined as potential mid-Carboniferous boundary stratotype sections (Lane and Manger 1985). From 1957 to 1983, a single Devonian through Pennsylvanian section at Granite Mountain (fig. 1) was sampled by U.S. Geological Survey (U.S.G.S.) workers for lithofacies and fossils, including cephalopods (Gordon and others 1984, 1985), brachiopods (Gordon and others 1984, 1985; Gordon and others 1982), conodonts (Wardlaw 1984), and calcareous foraminifers and algae (Gordon and others 1985; Mamet 1982, 1984).

This paper provides new data on the carbonate microfacies and related conodont abundances and conodont biofacies of the Mississippian-Pennsylvanian transition beds at Granite Mountain. In addition, the carbonate microfacies and conodont biofacies are placed within a depositional model for the lower Ely Limestone, and mid-Carboniferous conodonts previously reported from Granite Mountain are illustrated. The data given here are

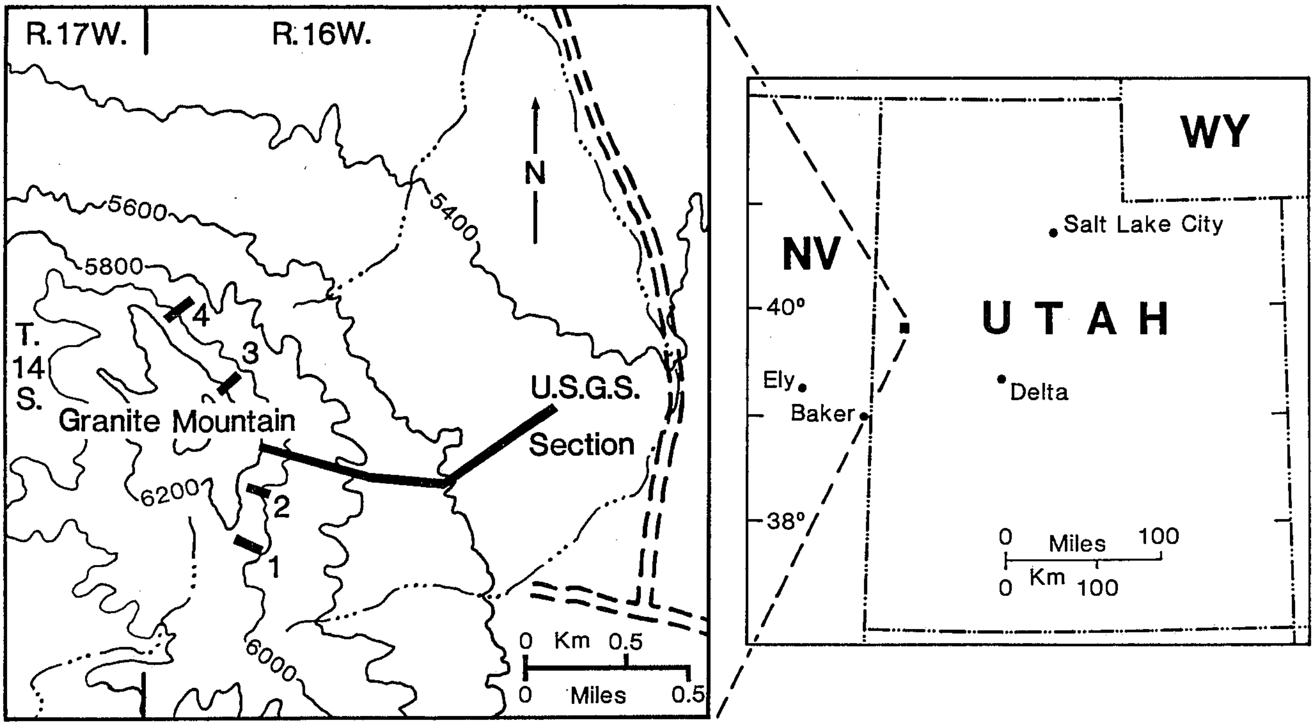

FIGURE 1.—*Location map of study area. Measured sections 1 to 4 are referred to in the text as GM-1 to GM-4, respectively. The U.S.G.S. section is that of Gordon and others (1984, 1985). The U.S.G.S. section extends from the top of the Pilot Shale (Upper Devonian) upward across the Chainman Shale (Mississippian) into the lower portion of the Ely Limestone (Upper Mississippian and Lower Pennsylvanian). Contour interval is 200 ft. Base is from U.S.G.S. Granite Mountain, Utah, 15-Minute Quadrangle. Detailed directions and mileages to the Granite Mountain exposure are given by Webster and others (1984).*

part of a larger study of the lithostratigraphy, lithofacies, brachiopod biostratigraphy, and conodont biostratigraphy of the Mississippian-Pennsylvanian boundary strata laterally adjacent to the U.S.G.S. section at Granite Mountain (Morrow 1989; Morrow and Webster 1989a, 1990).

Results are based on four 11- to 16-m-thick measured sections, designated GM-1 to GM-4 (fig. 1), which begin 36 to 40 m above the base of the Ely Limestone and extend upward across the Mississippian-Pennsylvanian boundary. A low dip, approximately 11° due west, allowed direct measurement of strata thickness using tape and ruler. A total of 150 conodont and oriented petrographic samples, at an average spacing of 35 cm, were taken from the four sections. Samples weighing 1 to 1.5 kg were processed for conodonts, except near conodont zone boundaries, where 2.0 to 3.0 kg samples were processed. Conodont samples were prepared using the procedure outlined by Collinson (1963), with the exception of dolomitic samples, which were dissolved in a 7% formic acid solution. Concentration of insoluble heavy residue containing conodonts was made using sodium polytungstate heavy liquid (Krukowski 1988, Savage 1988) following the cryogenic technique outlined by Merrill (1987) and Morrow and Webster (1989b). Illustrated specimens (pls. 1–4) are reposited in the U.S. National Museum under numbers 448916 to 448950.

STRATIGRAPHY AND CARBONATE MICROFACIES

A summary of the early nomenclatural history of the Ely Limestone is provided by Hose and Repenning (1959). Additional papers that reviewed previous stratigraphic, petrographic, paleogeographic, and tectonic studies of the Ely Limestone include Hose (1977), Rich (1977), St. Aubin-Hietpas (1983), and Welsh and Bissell (1979). A bibliography and summary of previous biostratigraphic work on the Ely Limestone is available in a field trip guidebook to the Mississippian-Pennsylvanian boundary in the eastern Great Basin (Webster and others 1984).

The Ely Limestone, which is as thick as 610 m in nearby Confusion Range sections (Hose 1974), forms a gently dipping erosional remnant capping Granite Mountain, where only the lower 215 m of the formation is present. Based on the lowest stratigraphic occurrence of the conodont *Declinognathodus noduliferus*, which is currently used to define the mid-Carboniferous boundary

(Lane and Manger 1985), the Mississippian-Pennsylvanian boundary occurs between 45 to 53 m above the base of the Ely Limestone at Granite Mountain. The Ely Limestone typically weathers into alternating cliff and slope topography. Resistant beds are composed of medium- to thick-bedded to massive grainstone, packstone, and wackestone that are separated by recessive-weathering, thin-bedded to laminated calcareous shales, lime mudstones, wackestones, and rarely packstones and grainstones. Bioturbation is a common feature in all lithologies, giving many beds a mottled appearance. Rarely, discrete burrows are visible. Recessive units containing intergranular lime mud commonly also contain quartz silt and very fine quartz sand. Locally, slope-forming beds contain abundant silicified brachiopods that weather out intact. Tabular cross-bedding and cross-laminations, enhanced by pressure solution and differential weathering, are visible within resistant grainstone units. These cross-strata have dips of 20° to 25° due east (corrected for bedding dip).

Massive, sucrosic dolomite is locally common in the lower Ely Limestone. In some dolomitized samples, determination of the precursor carbonate microfacies type was impossible due to diagenesis, although conodont recoveries from these same samples were similar to those of nondolomitized intervals. Chert nodules and lenses, which are rarely present below the systemic boundary, become very common in the Pennsylvanian portion of the Ely Limestone. Dolomite and silica replace a variety of skeletal grains, including echinoderms, bryozoans, and brachiopods. These diagenetic features are considered to have formed from shallow burial alteration of an essentially normal-marine limestone. Pressure-solution seams and stylolites, commonly enhanced by surface weathering, are also very common within wackestone, packstone, and grainstone units. Based on crosscutting relations, silicification predates dolomitization, which in turn predates pressure solution. Conodont color alteration index (CAI) values of 1½ to 2 were noted for conodont elements recovered in the study. Hose (1977) considers tectonic unloading of Paleozoic strata in the Granite Mountain area to have started no earlier than Late Jurassic (163 million years) and no later than early Oligocene (36.5 million years). This time frame, combined with Ahrrenius plots given by Epstein and others (1977), would correspond to a range of maximum burial temperatures from $< 50°$ C to near 65° C for the lower Ely Limestone.

CARBONATE MICROFACIES

Nine shallow-water marine carbonate microfacies are recognized in this study, representing a spectrum of depositional fabrics and textures ranging from lime mudstones to well-sorted skeletal grainstones. These microfacies are typically thin and varied, and commonly more than one microfacies type is present in a single thin section. Where multiple microfacies were observed in a single thin section, designation of microfacies types was based on the dominant lithology. For ease in plotting data on graphs, the carbonate microfacies are categorized using the Standard Microfacies Types (SMF Types) of Wilson (1975) as amplified by Flugel (1982), with the exception of the shallow-marine spiculite microfacies (SMF-1-S), which is adapted from Stevens and Armin (1983). In addition, Wilson SMF-11 is further subdivided into types 11f (fine grained) and 11c (coarse grained), based on the dominant allochem size. Where possible, relict fabrics, silicified fossils, and conodonts were used to tentatively assign dolomitized samples to SMF Types. Several dolostone samples (e.g., GM-2 2.48, 3.20, and 3.83) yielded abundant conodonts, commonly 60 or more platform (Pa) elements per kg of sample. Where these conodont abundances are found in nondolomitized samples, the rock belongs to the bioclast packstone and grainstone microfacies (SMF-12). Similar conodont abundances, combined with preserved original depositional textures and fabrics from thin section and field observation, were used to infer microfacies types in samples where primary texture was obscured or destroyed by dolomitization. Grain and crystal abundances, given relative to total sample or thin section, are described as follows: rare = less than 2%; common = 2 to 20%; abundant = 21 to 50%; and dominant = greater than 50%.

Shallow-Marine Spiculite Microfacies (SMF-1-S)

Description. The shallow-marine spiculite microfacies (fig. 2) includes lime mudstone with subsidiary wackestone and nodular calcareous shale. This microfacies is sparsely fossiliferous except for sponge spicules, which are common to abundant, and rare concentrations of bivalves and large, whole productid brachiopods (dominantly silicified). Sponge spicules are generally scattered, and rarely dense concentrations of interwoven spicules are present. Spicules appear leached and calcite-replaced, with relict central tubes and triaxon forms rarely preserved. Other skeletal grains present include (1) rare to common ostracodes and echinoderms; and (2) rare trilobites, bryozoans, and calcareous algae. Conodont faunas from this microfacies are low in both diversity and abundance, being dominated by *Adetognathus lautus*. Conodont element abundances are less than 8 Pa elements per kg of sample.

The matrix of this microfacies is composed of lime mud that locally grades to recrystallized microspar. Microspar is typically concentrated along individual laminae. Relict fenestral porosity and burrow structures commonly disrupt lamination. Burrows are distinguished by wackestone-filled patches with concentrations of 0.05 to 1.0 mm skeletal grains, mud pellets, and lumps. Very rarely, the spiculite microfacies fills subvertical burrows and forms intraclasts in adjacent grainstone microfacies. Rare geopetal fill was observed within whole bivalves. Angular quartz silt and angular to subangular very fine quartz sand are common to locally abundant within the matrix, both as scattered grains and concentrations along laminae. SMF-1-S forms weakly to moderately resistant outcrops that are thin-bedded to irregularly laminated, or massive when bioturbated.

Occurrence. The shallow-marine spiculite microfacies composes 3% of Granite Mountain section GM-2, and 2% of Granite Mountain section GM-3. This microfacies was not noted in Granite Mountain sections GM-1 or GM-4.

Bioclast Wackestone Microfacies (SMF-9)

Description. The bioclast wackestone microfacies (fig. 3) contains a wide variety of poorly sorted, 0.05 to 50 mm wide skeletal grains in low to moderate abundance floating in a matrix-supported fabric. Commonly, this microfacies contains bioclast packstone patches where bioturbation has concentrated skeletal debris. In several samples, this microfacies is gradational to SMF-1-S, the shallow-marine spiculite microfacies. Varied amounts of disarticulated and fragmented skeletal grains are present, with sporadic concentrations of whole fossils. Skeletal grains are composed of (1) common to locally abundant spinose brachiopods, ostracodes, fenestrate bryozoans, and ramose bryozoans; (2) common echinoderms; (3) rare to common mollusks, calcareous foraminifers, and calcareous algae; and (4) rare trilobites, sponge spicules, and phosphatic skeletal debris. Conodont abundances in SMF-9 range from 3 to 15 Pa elements per kg of sample. Locally, distinct micrite-filled macroborings are present on bioclast margins.

Abundant to dominant lime mud is present as matrix, commonly with angular to subangular quartz silt and fine quartz sand. Locally, lime mud pellets are concentrated by bioturbation, and minor calcite spar-filled porosity is present around allochems and within fenestral voids. Intragranular porosity is dominantly calcite spar filled, except for rare geopetal fill within larger whole shell debris. Compaction features include common pressure-solution seams, defined by concentrations of insoluble residue, and rare microstylolites. Opaque minerals, occurring in the matrix as scattered grains and localized patches, include very fine to medium crystalline hematite, limonite, and hematite after pyrite. SMF-1-S forms thin and nodular to massive beds that are weakly to moderately resistant.

Occurrence. The bioclast wackestone microfacies composes 39% of Granite Mountain section GM-3, 28% of Granite Mountain section GM-2, 27% of Granite Mountain section GM-1, and 23% of Granite Mountain section GM-4.

Coated and Worn Bioclast Packstone Microfacies (SMF-10)

Description. The coated and worn bioclast packstone microfacies (fig. 4) consists of abundant, poorly sorted, micrite-coated, and worn 0.05- to 0.5-mm-wide skeletal debris with an open, grain-supported fabric. Rare skeletal debris as much as 5 mm across is also present. Bioturbation locally concentrates coated allochems and intergranular lime mud, giving a mottled wackestone-packstone texture. Crude lamination and micrograding of allochems are rarely present in nonburrowed intervals. Skeletal components of this microfacies include (1) common to abundant echinoderms; (2) common brachiopods, ramose bryozoans, and calcareous algae fragments (preserved as micrite envelopes and rarely encrusting as oncoids); and

EXPLANATION OF PLATE 1

Figs. 1–3.—*Adetognathus unicornis* (Rexroad and Burton). Pa element; oral, aboral, and lateral views; GM-3 1.06 m, USNM 448916, X70. Figs. 4–6.—*Adetognathus lautus* (Gunnell). Pa element; oral, aboral, and lateral views; GM-3 12.37 m, USNM 448917, X70. Figs. 7–9.—*Adetognathus lautus* (Gunnell). Pa element; oral, aboral, and lateral views; GM-2 9.30 m, USNM 448918, X70. Figs. 10–11.—*Adetognathus lautus* (Gunnell)/ *Adetognathus spathus* (Dunn) transitional sp. Pa element; oral and lateral views; GM-3 15.42 m, USNM 448919, X70. Figs. 12–13.—*Adetognathus spathus* (Dunn). Pa element; oral and lateral views; GM-3 14.07 m, USNM 448920, X70. Figs. 14–16.—*Adetognathus spathus* (Dunn). Pa element; oral, aboral, and lateral views; GM-3 14.79 m, USNM 448921, X70.

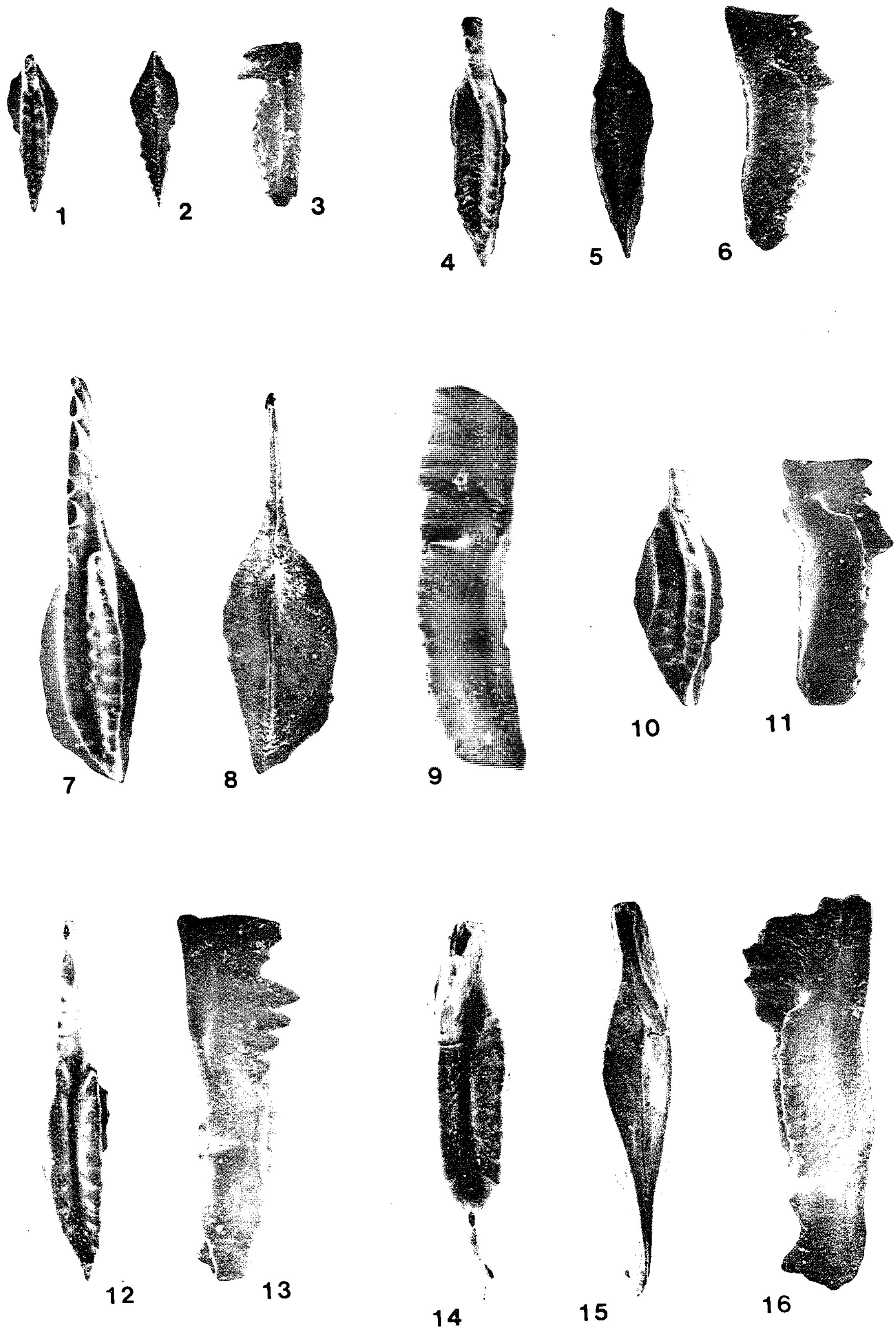
1
2
3
4
5
6
7
8
9
10
11
12
13
14
15
16

(3) rare trilobites, mollusks, foraminifers, sponge spicules, ostracodes, and phosphatic skeletal debris. Conodont abundances in SMF-10 are quite varied, ranging from 4 to 35 Pa elements per kg of sample. Many skeletal fragments are surrounded by micrite-filled macroborings. Nonskeletal components include rare to locally common lime mudstone and wackestone intraclasts, mud pellets (gradational to totally micritized grains), and poorly formed ooids. Ooids rarely show more than three discrete growth bands and are dominantly micrite coated.

The matrix of this microfacies is composed primarily of lime mud, with rare scattered angular quartz silt and angular to subangular very fine quartz sand. Rare shelter voids are present beneath large skeletal grains, and rotated geopetal fabric is noted within whole bivalved fossils. Occasional sutured stylolite grain contacts, rare pressure-solution seams, and rare shattered micrite envelopes (calcareous algae molds) are present. Rare coarsely crystalline or smaller opaque grains, typically weathered to limonite or hematite, are also visible. SMF-10 forms medium to thick and massive beds that are commonly resistant and well exposed.

Occurrence. The coated and worn bioclast packstone microfacies composes 24% of Granite Mountain section GM-3, 23% of Granite Mountain section GM-1, 19% of Granite Mountain section GM-4, and 10% of Granite Mountain section GM-2.

Fine-Grained, Coated Bioclast Grainstone Microfacies (SMF-11f)

Description. Flugel (1982) defined SMF Type 11 as a grainstone containing coated bioclasts in a sparry cement. In thin sections of the present study, this microfacies occurs in two end-member types based on dominant grain size: a fine-grained grainstone microfacies (herein designated SMF-11f) and a coarse-grained grainstone microfacies (herein designated SMF-11c). The fine-grained coated bioclast grainstone microfacies (fig. 5) is characterized by tightly packed, moderately to well-sorted bioclasts in the 0.1 to 0.4 mm grain size range. Skeletal grains larger than 0.4 mm are conspicuously rare, composing less than 5% of the total sample. Bioclasts in SMF-11f include (1) common brachiopods, echinoderms, bryozoans, and calcareous algae (preserved as calcite-filled micrite envelopes and encrusting as oncoids); and (2) rare mollusks, foraminifers, trilobites, ostracodes, phosphatic skeletal fragments, and lime mudstone intraclasts. Conodonts in this microfacies are fairly abundant, ranging from 10 to 45 Pa elements per kg of sample. Bioclasts are dominantly lime-mud coated and plugged and appear worn and fragmented. Rare pellets, gradational to totally micritized skeletal fragments, are also present. In addition, distinct lime-mud filled macroborings are locally present.

Vague horizontal laminations, defined by orientation of elongate grains parallel to bedding and concentrations of single-sized grains within individual laminae, are common. Bioturbation uncommonly disrupts lamination. Rare intergranular lime mud forms laminae, patches, and shelter void fabrics. Intergranular voids are dominantly filled with crystalline, equant, and syntaxial rim cements, except for sporadic micrite matrix, noted above, and rare subangular quartz silt and very fine quartz sand. Intragranular space is mostly mud filled, with rare silica replacement, and hematite and/or hematite after pyrite.

EXPLANATION OF PLATE 2

Fig. 1.—*Adetognathus spathus* (Dunn). Pa element; lateral view of platform and posterior blade; GM-1 9.74 m, USNM 448922, X70. Figs. 2–4.—*Adetognathus spathus* (Dunn). Pa element; oral, aboral, and lateral views; GM-3 15.27 m, USNM 448923, X70. Figs. 5–6.—*Adetognathus* sp. cf. *Adetognathus* n. sp. Tynan (1980). Pa element; oral and lateral views; GM-2 3.20 m, USNM 448924, X70. Figures 7–17 are ramiform elements associated with Pa elements of *Adetognathus lautus* and *Adetognathus spathus*. Fig. 7.—Pb element; lateral view; GM-3 15.27 m, USNM 448925, X40. Fig. 8.—Pb element; lateral view; GM-3 15.27 m, USNM 448926, X40. Fig. 9.—Sa element; lateral view; GM-1 9.74 m, USNM 448927, X40. Fig. 10.—Sa element; posterior view; GM-3 15.42 m, USNM 448928, X40. Fig. 11.—M element; lateral view; GM-3 15.42 m, USNM 448929, X40. Fig. 12.—M element; lateral view; GM-1 9.74, USNM 448930, X40. Fig. 13.—M element; lateral view; GM-1 9.33 m, USNM 448931, X40. Fig. 14.—Sc element; posterior process; GM-1 9.33 m, USNM 448932, X40. Fig. 15.—Sc element; posterior process; GM-1 9.33 m, USNM 448933, X40. Fig. 16.—Sc element; lateral process and anterior cusp; GM-1 9.33 m, USNM 448934, X40. Fig. 17.—Sc element; lateral process and anterior cusp; GM-2 8.82 m, USNM 448935, X40. Figs. 18–19.—Broken specimen assignable to either *Adetognathus* sp. or *Rhachistognathus* sp. Pa element; oral and lateral views; GM-1 2.87 m, USNM 448936, X70.

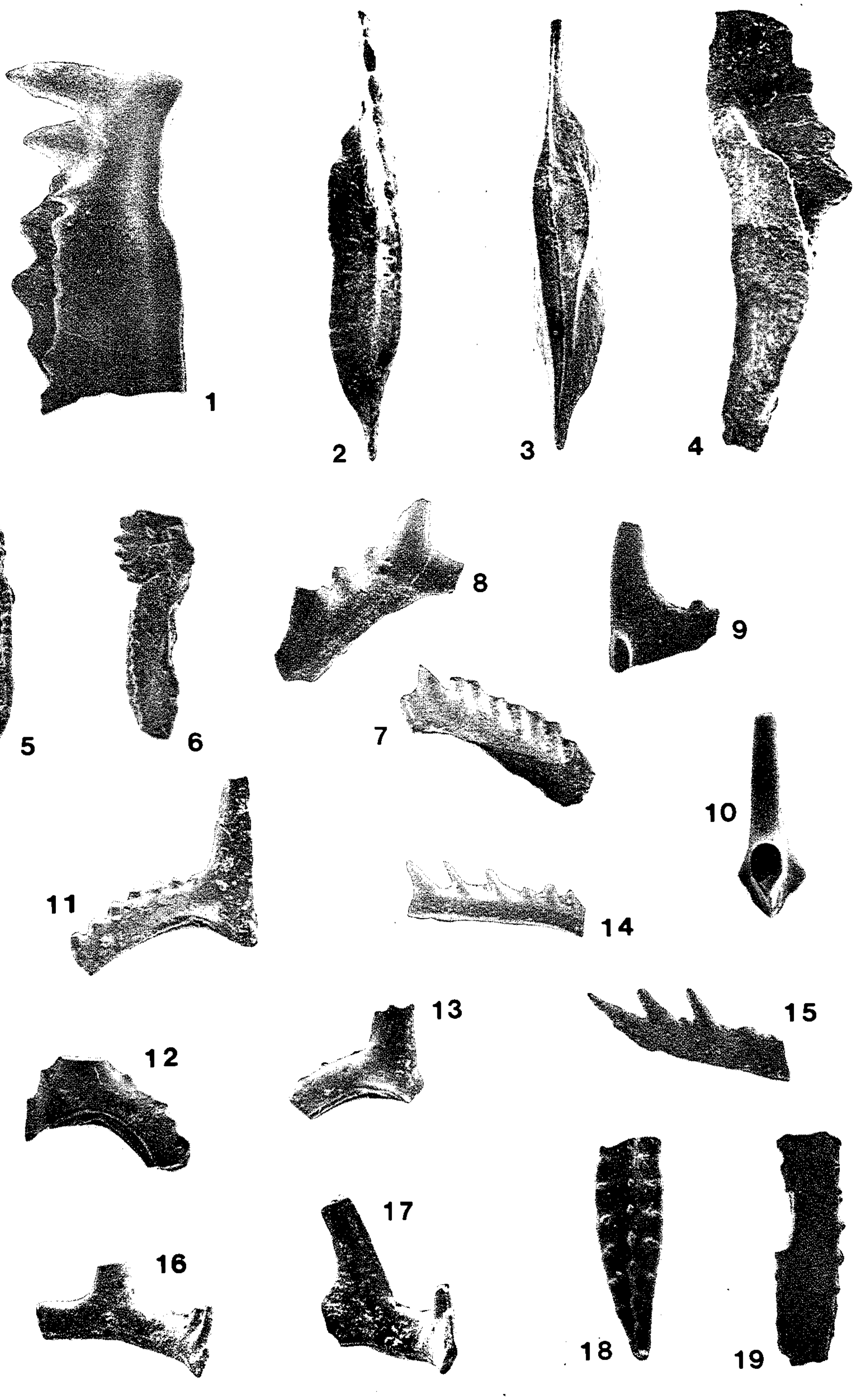
1
2
3
4
5
6
7
8
9
10
11
12
13
14
15
16
17
18
19

Micrite envelopes formed around calcareous algae are rarely flattened, and occasional stylolites and sutured grains occur. In the field, this microfacies is found in well-exposed beds of varied thickness, usually medium to thick bedded, showing common cross-bedding and cross-lamination.

Occurrence. The fine-grained coated bioclast grainstone microfacies composes 9% of Granite Mountain section GM-3, 3% of Granite Mountain section GM-1, and 2% each of Granite Mountain sections GM-2 and GM-4.

Coarse-Grained, Coated Bioclast Grainstone Microfacies (SMF-11c)

Description. The coarse-grained, coated bioclast grainstone microfacies (fig. 6) is characterized by an open, moderately well-sorted fabric with abundant mud-coated, mud-plugged, and abraded allochems. Grains in SMF-11c range from 0.3 to 10 mm in diameter. Allochems in SMF-11c are composed of (1) common to abundant echinoderms; (2) common brachiopods, bryozoans, trilobites, calcareous algae (preserved as micrite envelopes and rarely forming oncoids), and intraclasts; and (3) rare ostracodes, phosphatic skeletal debris, pellets, and ooids. In contrast to SMF-11f, conodonts in SMF-11c are rare, with abundances of 0 to 5 Pa elements per kg of sample. Ooids are mud coated and typically abraded. Intraclasts are composed of a variety of rock types, including pellet and spiculite lime mudstone (SMF-1-S), laminated lime mudstone, bioclast wackestone (SMF-9), and bioclast packstone (SMF-10). Very rare authigenic alkalai feldspar laths are present within some lime mudstone intraclasts.

Intergranular voids are filled with calcite spar, largely as coarsely crystalline syntaxial rim cements on echinoderm grains, and rarely as acicular isopachous rinds on other skeletal grains. Crude lamination is formed by concentrations of similar-sized grains within single layers and orientation of elongate skeletal fragments parallel to bedding. Mud-filled macroborings are rarely present on allochem margins, and geopetal fabric is rarely noted within micrite envelopes formed around calcareous algae grains. Compaction features include common flattened micrite envelopes and stylolites. Stylolite surfaces generally show as much as 2.5 mm of relief. Rare pyrite and hematite after pyrite are also present. This microfacies is present in well-exposed, medium to thick beds showing tabular cross-bedding and cross-lamination.

Occurrence. The coarse-grained, coated bioclast grainstone microfacies composes 17% of Granite Mountain section GM-1, 12% of Granite Mountain section GM-3, and 5% each of Granite Mountain sections GM-2 and GM-4.

Bioclast Packstone and Grainstone Microfacies (SMF-12)

Description. The bioclast packstone and grainstone microfacies (fig. 7) consists of poorly sorted, 0.05 to 15 mm wide allochems in a tightly packed, grain-supported fabric. Concentrations of larger, disarticulated brachiopod shells are locally present. Although typically mud coated and fragmented, bioclasts usually do not show evidence of extensive abrasion or wear. Bioclast composition is locally dominated by a single fossil group, primarily echinoderms and codiacean and/or dasycladacean green algae. Other grains in SMF-12 include common brachiopods, foraminifers, and ramose bryozoans. Rare mollusks, ostracodes, trilobites, phosphatic skeletal fragments, and wackestone/lime mudstone intraclasts are also present. Distinct micrite-filled macroborings are commonly preserved on trilobite fragments. Samples of this microfacies

EXPLANATION OF PLATE 3

Figs. 1–3.—*Cavusgnathus unicornis* Youngquist and Miller. Pa element; oral, aboral, and lateral views; GM-3 1.70 m, USNM 448937, X70. Figs. 4–5.—*Hindeodus minutus* (Ellison). Pa element; oral and lateral views; GM-3 1.70 m, USNM 448938, X70. Figs. 6–7.—*Gnathodus defectus* Dunn. Pa element; oral and lateral views; GM-1 7.40 m, USNM 448939, X70. Fig. 8.—*Gnathodus girtyi simplex* Dunn. Pa element; oral view; GM-3 1.70 m, USNM 448940, X70. Fig. 9.—*Gnathodus girtyi girtyi* Hass. Pa element; oral view; GM-2 0.90 m, USNM 448941, X70. Fig. 10.—*Gnathodus bilineatus* (Roundy). Pa element; oral view; GM-1 1.77 m, USNM 448942, X70. Figs. 11–13.—*Declinognathodus noduliferus* (Ellison and Graves). Pa element; oral, aboral, and lateral views; GM-4 11.49 m, USNM 448943, X70. Figs. 14–15.—*Rhachistognathus websteri* Baesemann and Lane. Pa element; oral and lateral views; GM-3 14.79 m, USNM 448944, X70.


1
2
3
4
5
6
7
8
9
10
11
12
13
14
15

produced the greatest abundances of conodonts recovered in the study, with yields as high as 125 Pa elements per kg of sample.

Intergranular lime mud is variably present, with the bulk of remaining space between grains filled with blocky, medium to coarsely crystalline syntaxial cement formed around echinoderm ossicles. Rare subangular quartz silt and very fine quartz sand occurs within the matrix. Intragranular porosity is filled with both micrite and finely crystalline calcite spar in about equal amounts, and rare geopetal fabric is observed. Stylolites and sutured grain boundaries are common, being marked by concentrations of insoluble residue. Common coarsely crystalline or finer opaque crystals, including hematite, limonite, hematite after magnetite, and hematite after pyrite, are found plugging mud-filled intragranular voids and are rarely concentrated along stylolites. This microfacies type forms thick, well-exposed, resistant beds.

Occurrence. The bioclast packstone and grainstone microfacies composes 45% of Granite Mountain section GM-2, 39% of Granite Mountain section GM-4, 18% of Granite Mountain section GM-1, and 11% of Granite Mountain section GM-3.

Lag Microfacies (SMF-14)

Description. The lag microfacies (fig. 8) is characterized by a moderately well-sorted, open grain-supported fabric containing 0.25- to 15-mm-wide allochems dominated by rounded intraclasts and fragmented, worn, mud-coated, and mud-filled skeletal grains. Allochems in SMF-14 include common to abundant intraclasts, echinoderm ossicles, and brachiopods. Locally, ooids and calcareous algae (preserved as spar-filled micrite envelopes and oncoids) are also common. Rare grains include ramose bryozoans, mollusks, lime mud lumps, and lime mud pellets. Conodont abundances are low, less than 5 Pa elements per kg of sample, and abraded elements are common. The intraclasts in this microfacies show a wide variety of composition, including (1) bioclast and ooid wackestone; (2) massive, microlaminated, and pelletal lime mudstone (occasionally containing foraminifers and calcareous algae); (3) pale green, silty, calcareous mudstone; (4) and quartz-rich calcareous siltstone.

Primary intergranular porosity, initially quite high, is now filled with coarsely crystalline calcite spar, composed predominantly of syntaxial rim cements surrounding echinoderm fragments. Rare acicular isopachous calcite fringes, possibly preserving marine cements, are present on some brachiopod and mollusk fragments. Common angular to subangular quartz silt and very fine quartz sand are locally present within intragranular micrite. Fractured micrite envelopes are common, and stylolites with sutured grain boundaries are rare. Authigenic medium crystalline hematite, hematite after pyrite, and hematite rinds are common within and around fine-grained intraclasts. In the field, this microfacies occurs in moderately well-exposed, medium beds that are massive internally and bounded by sharp contacts. Typically, these beds are variable in thickness and pinch out when traced laterally. Local concentrations of coarse bioclast debris are present, and common mud-rich intraclasts give the microfacies a mottled, dark gray texture.

Occurrence. The lag microfacies composes 2% of Granite Mountain section GM-3 and 1% of Granite Mountain section GM-4. This microfacies was not noted in Granite Mountain sections GM-1 or GM-2.

Ooid Grainstone Microfacies (SMF-15)

Description. The ooid grainstone microfacies (fig. 9) is dominated by poorly developed, well-sorted, 0.1- to 1.0-mm-wide ooids in a moderately packed, grain-supported fabric. Ooids generally show three or less distinct cortices

EXPLANATION OF PLATE 4

Figs. 1–2.—*Rhachistognathus muricatus* (Dunn). Pa element; oral and lateral views; GM-3 3.81 m, USNM 448945, X70. Figs. 3–5.—*Rhachistognathus muricatus* (Dunn). Pa element; oral, aboral, and lateral views; GM-3 3.81 m, USNM 448946, X70. Figs. 6–8.—*Rhachistognathus muricatus* (Dunn)/ *Rhachistognathus primus* Dunn transitional sp. Pa element; oral, aboral, and lateral views; GM-3 2.52 m, USNM 448947, X70. Figs. 9–10.—*Rhachistognathus primus* Dunn. Pa element; oral and lateral views; GM-2 7.40 m, USNM 448948, X70. Figs. 11–13.—*Rhachistognathus primus* Dunn. Pa element; oral, aboral, and lateral views; GM-2 7.40 m, USNM 448949, X70. Figs. 14–15.—*Rhachistognathus prolixus* Baesemann and Lane. Pa element; oral and lateral views; GM-3 11.53 m, USNM 448950, X70.

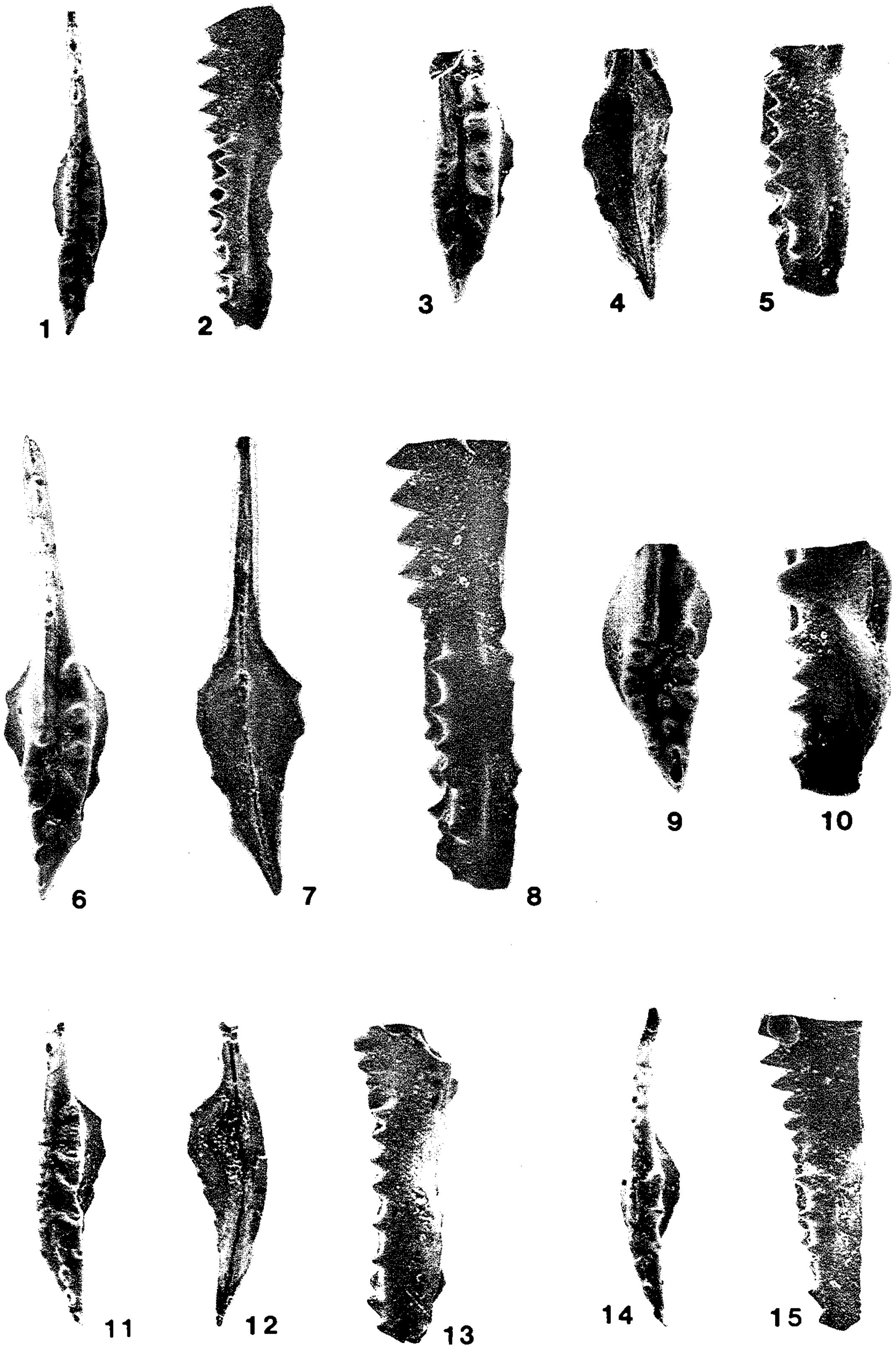
1
2
3
4
5
6
7
8
9
10
11
12
13
14
15

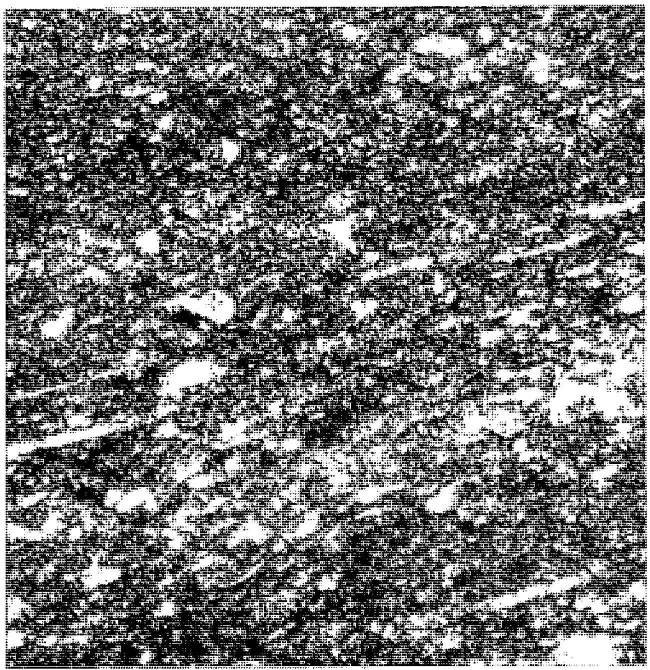

FIGURE 2.—*Photomicrograph of shallow-marine spiculite microfacies, SMF-1-S. Sample GM-2 8.00 m; field of view is 1.0 mm.*

FIGURE 3.—*Photomicrograph of bioclast wackestone microfacies, SMF-9. Sample GM-3 3.31 m; field of view is 1.0 mm.*

and often are mud coated to mud filled. Typically, the ooids are concentrated within laminations and cross-laminations, alternating with micrite-rich horizons. Rare burrows, now filled with coarsely crystalline calcite spar, are also present. Skeletal fragments, present both as discrete grains and ooid cores, are composed of (1) common to abundant calcareous algae (preserved as micrite envelopes and as oncoids), echinoderms, and ostracodes; and (2) rare mollusks, brachiopods, bryozoans, trilobites, spicules, and phosphatic skeletal grains. Conodonts are variably and locally abundant, with yields ranging from 6 to 55 Pa elements per kg of sample. Also present are pellets and intraclasts. The intraclasts, which rarely form ooid cores, are composed of lime mudstone, spiculite mudstone (SMF-1-S), wackestone (SMF-9), and rare pale green calcareous siltstone.

Lime mud laminations occur locally within SMF-15. Rare angular to subangular silt and very fine quartz sand are present between grains. Remaining intergranular voids are filled with (1) finely crystalline granular calcite cement; (2) coarsely crystalline blocky syntaxial rim cement around echinoderm grains; and (3) rare isopachous acicular calcite cement (after marine cement?) coating ooids. Occasionally, incipient silicification of ooid cortices is present. Rare hematite and hematite after pyrite fill intragranular void space. Stylolites and sutured grains are common, and ooids only rarely show evidence of fracture or compaction. In the field, SMF-15 occurs in thin, well-exposed beds commonly bounded by calcareous shale partings. Internally, vague laminations, cross-laminations, and subvertical burrows are visible.

Occurrence. The ooid grainstone microfacies composes 2% of Granite Mountain section GM-2. This microfacies is absent in Granite Mountain sections GM-1, GM-3, and GM-4.

Pellet and Lump Packstone Microfacies (SMF-16/17)

Description. The pellet and lump packstone microfacies (fig. 10) consists of a poorly sorted, open, skeletal, grain-supported fabric with common to abundant micrite pellets and lumps. Wilson (1975) and Flugel (1982) originally recognized SMF-16 and SMF-17 as two separate grainstone microfacies defined by the dominance of lime mud pellets or aggregrate lumps, respectively. Samples referred to as SMF-16/17 in the present study contain intergradational lime mud pellets and lumps that occur with common intergranular micrite. Grains range from 0.1 to 50 mm in diameter, and lumps as wide as 0.25 mm are present. Bioclasts are dominantly mud coated (often filling distinct macroborings on grain margins) and mud filled and contain occasional whole bivalves, brachiopods, and gastropods. Skeletal grains only rarely show evidence of abrasion or rounding. Allochems in SMF-16/17 are composed of (1) common to abundant calcareous algae (primarily discrete segments preserved by micrite en-

FIGURE 4.—*Photomicrograph of coated and worn bioclast packstone microfacies, SMF-10. Sample GM-3 2.35 m; field of view is 1.0 mm.*

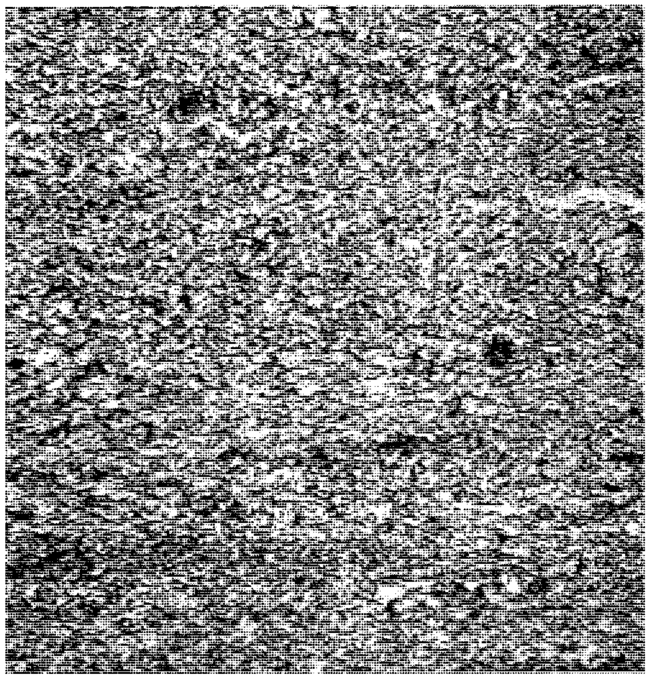

FIGURE 5.—*Photomicrograph of fine-grained coated bioclast grainstone microfacies, SMF-11f. Sample GM-3 1.06 m; field of view is 20 mm.*

velopes, and rare oncoids); (2) common brachiopods, mollusks, echinoderms, bryozoans, and ostracodes; and (3) rare foraminifers, trilobites, phosphatic skeletal debris, leached sponge spicules, and lime mudstone/wackestone intraclasts. Conodont abundances in this microfacies are variable, ranging from 0 to 30 Pa elements per kg of sample. Diversity is generally low, with species of *Adetognathus* dominating the fauna. Rarely, species of *Rhachistognathus* occur in abundances of less than 10 Pa elements per kg of sample.

Intergranular space is filled with approximately 50% lime mud pellets and/or lumps, with remaining space filled by calcite spar consisting of coarse, blocky, syntaxial rim cement surrounding echinoderm grains. Rarely, syntaxial rim cement is lacking around echinoderm fragments. Where this occurs, echinoderm grains are armored by micrite rims that apparently prevented growth of syntaxial cement. Crude lamination is suggested by orientation of elongate bioclasts parallel to bedding. Pelletal mud-filled burrows are occasionally visible. Common calcite mosaic-filled molds after calcareous algae, mollusks, and spicules are also present. Geopetal and shelter void fabrics are rarely noted, and fenestral voids occur within some micrite patches. Common fractured micrite envelopes and stylolites (with up to several centimeters of relief) are present. Rare hematite and hematite after pyrite plugs intragranular porosity and is concentrated along stylolites. In the field, this microfacies has fair to good exposure, with beds of variable thickness. Beds typically show irregular, wispy, black lime mud laminations, pelletal patches, and crude bioclast laminations.

Occurrence. The pellet and lump packstone microfacies composes 5% of Granite Mountain sections GM-2 and GM-4, 3% of Granite Mountain section GM-1, and 1% of Granite Mountain section GM-3.

CONODONT BIOFACIES

Previous biostratigraphic studies utilizing Carboniferous conodont data from the Granite Mountain–Confusion Range area include Dunn (1970a), Gordon and others (1984), Sandberg and others (1980), Tynan (1980), Wardlaw (1984), and Webster and others (1984). Early works proposing Carboniferous conodont biofacies models and paleoecologic interpretations of the conodont animal include those of Barnes and others (1973), Druce (1973), Merrill (1973), Merrill and von Bitter (1976), Seddon and Sweet (1971), and von Bitter (1972). Subsequent studies, including Austin and Davies (1984), Davis and Webster (1985), Driese and others (1984), Merrill and von Bitter (1984), Sandberg and Gutschick (1984), and von Bitter and others (1986), have further refined Carboniferous conodont biofacies and the environmental controls affecting conodont abundance and distribution patterns. Physical and chemical factors such as water depth, water temperature, hydraulic energy, pH, salinity, and biotic

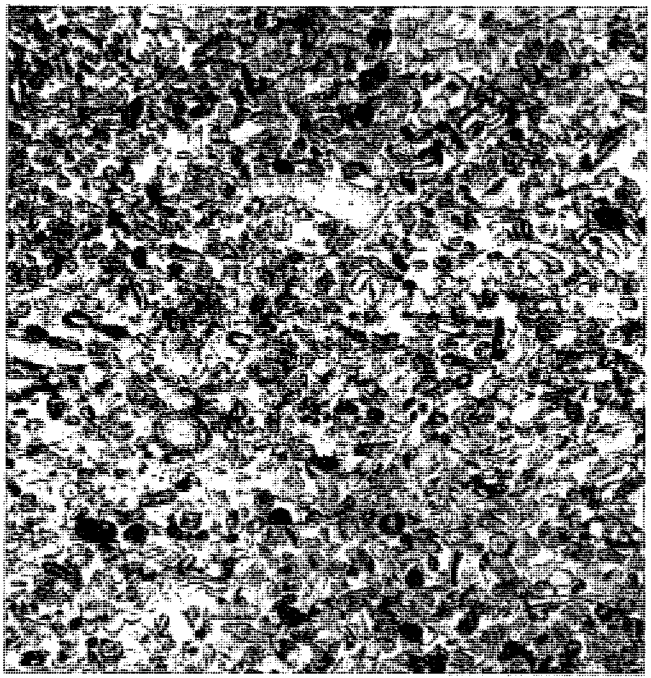

FIGURE 6.—*Photomicrograph of coarse-grained, coated bioclast grainstone microfacies, SMF-11c. Sample GM-3 9.40 m; field of view is 20 mm.*

FIGURE 7.—*Photomicrograph of bioclast packstone and grainstone microfacies, SMF-12. Sample GM-3 11.53 m; field of view is 20 mm.*

association have all been cited as parameters that affect substrate type and could have influenced the distribution of the living conodont animal. In addition, postmortem factors such as hydraulic sorting, winnowing, and transport clearly have affected the distribution of conodont elements, especially given the shallow water and locally high-energy conditions that prevailed in many Carboniferous depositional environments.

In the present study, a total of 15 previously described conodont species representing 6 genera were identified from the Mississippian-Pennsylvanian boundary strata at Granite Mountain (pls. 1–4). Overall, these conodont faunas are dominated by the genus *Adetognathus* and the closely allied genus *Cavusgnathus*, which compose 63% of the 4200 Pa elements recovered. In decreasing abundance, other conodont genera recovered include *Rhachistognathus* (33%), *Gnathodus* (2%), *Declinognathodus* (1%), and *Hindeodus* (<1%).

For each of the Granite Mountain measured sections, a plot of corresponding SMF Types, inferred relative shoreline position, and conodont abundances was made (figs. 11–14). These plots show a complex pattern of conodont occurrences that appear intimately tied to small-scale, cyclic changes in lithology. Conodont faunas typically show the dominance of a single genus over other genera in any given interval. The alternating and recurring dominance of the genera *Adetognathus* and *Rhachistognathus* define two previously proposed mid-Carboniferous conodont biofacies: (1) the *Adetognathus* biofacies and (2) the *Rhachistognathus* biofacies. Elements of *Gnathodus* and *Declinognathodus* do not occur in sufficient abundance to allow recognition of other proposed Carboniferous biofacies defined by the dominance of these genera.

ADETOGNATHUS BIOFACIES

Following Davis and Webster (1985) and Webster (1984), among others, the genus *Adetognathus* is considered to have evolved from the Mississippian genus *Cavusgnathus* sensu stricto, and both genera are inferred to have thrived in similar nearshore environments. The *Adetognathus* biofacies, defined by the dominance of species of the name-bearer, is considered ecologically equivalent to, and descendant from, the earlier Mississippian *Cavusgnathus* biofacies. In addition, the *Adetognathus* biofacies is equated to the Pennsylvanian *Cavusgnathus* biofacies described by Merrill (1973), Merrill and Martin (1976), and Merrill and von Bitter (1976).

The *Adetognathus* biofacies occurs repeatedly throughout all sections at Granite Mountain. This biofacies is characterized by a dominance of *Adetognathus lautus*, *A. spathus*, and, in the lower portions of the measured sections, *A. unicornis* and *Cavusgnathus unicornis*. Consistent with Davis and Webster (1985), the *Adetognathus* biofacies is inferred to have occurred in low-energy lagoon and tidal-flat environments that were

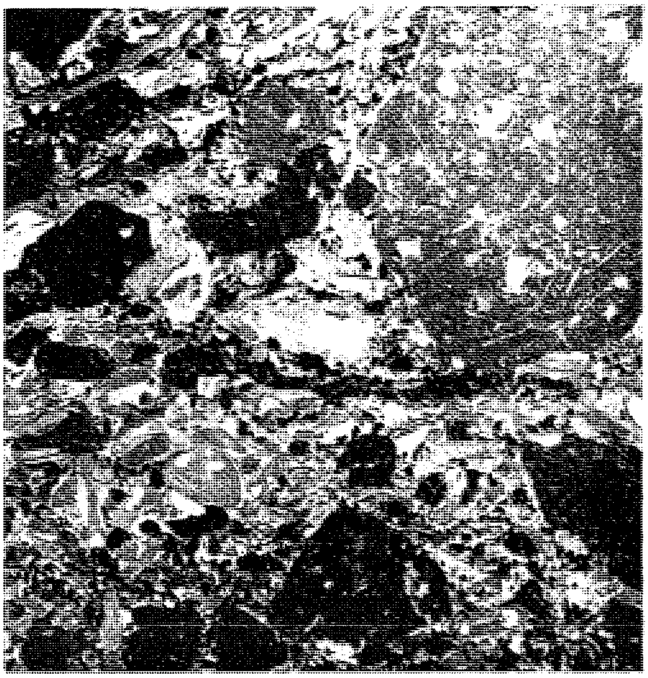

FIGURE 8.—*Photomicrograph of lag microfacies, SMF-14. Sample GM-3 0.30 m; field of view is 20 mm.*

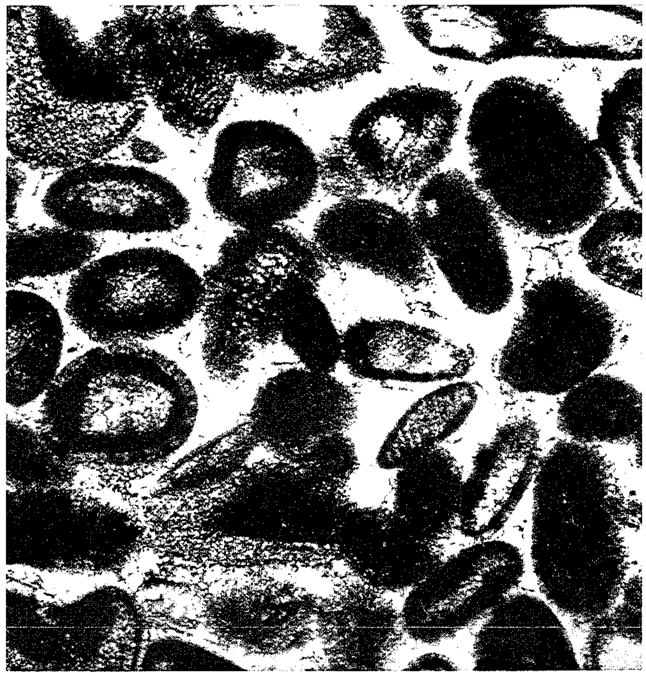

FIGURE 9.—*Photomicrograph of ooid grainstone microfacies, SMF-15. Sample GM-2 0.75 m; field of view is 1.0 mm.*

possibly subject to variable salinities. In addition, the partially protected, shoreward side of barrier bars or shoals may have favored this biofacies as well. This environment corresponds with: (1) all of the shallow-marine spiculite (SMF-1-S) and the pellet and lump packstone (SMF-16/17) microfacies; and (2) part of the bioclast wackestone (SMF-9), coated and worn bioclast packstone (SMF-10), fine-grained coated bioclast grainstone (SMF-11f), bioclast packstone and grainstone (SMF-12), and ooid grainstone (SMF-15) microfacies. Within these lithologies, species of *Adetognathus* and *Cavusgnathus* either dominate other species or are the only conodonts present, as in microfacies SMF-1-S. Associated biota within the *Adetognathus* biofacies include: (1) locally abundant calcareous algae (encrusting, dasycladacean, and codiacean), sponge spicules, mollusks, foraminifers, echinoderms, and brachiopods (especially spiriferids in packstone and productids in wackestone facies); and (2) locally common to rare bryozoans, ostracodes, and trilobites.

RHACHISTOGNATHUS BIOFACIES

There is less agreement among authors regarding the phylogenetic origin, and hence possible biofacies equivalents, of the genus *Rhachistognathus*. In erecting the genus *Rhachistognathus* and its type species *R. prima* (=*R. primus* of this report), Dunn (1966) considered the type species to have descended from the species *muricata* (=*R. muricatus*), which he had originally assigned to the genus *Cavusgnathus*. Webster (1969) has suggested that *Gnathodus muricatus* (=*R. muricatus*) developed from *Gnathodus girtyi simplex* stock in the late Chesterian. Alternatively, *G. muricatus* may have developed from *Spathognathodus* (=*Hindeodus*) by the addition of lateral parapets (Webster 1969). Dunn (1970b) later proposed that *Rhachistognathus* evolved from *Gnathodus commutatus commutatus* stock in the late Chesterian. Tynan (1980) considered *Rhachistognathus muricatus* and *R. primus* to have evolved from a Chesterian form termed *Rhachistognathus* sp. B. A similar conclusion was reached by Baesemann and Lane (1985), who considered the *muricatus* group (including *R. muricatus, R. primus,* and *R. websteri*) to have developed from an older *R. prolixus* stock in the late Chesterian. In the Baesemann and Lane (1985) report, *Rhachistognathus* sp. B of Tynan (1980) was placed in synonymy with *R. prolixus*. Possible predecessors of *R. prolixus* were not discussed by either Baesemann and Lane (1985) or Tynan (1980). In the present study, evidence of a phylogenetic source for *Rhachistognathus* is not present, as the genus is already firmly established in the lowest samples of the measured sections.

As noted by Davis and Webster (1985), Rafuse (1973), and Webster (1984), *Rhachistognathus* faunas dominate in shallow, often high-energy zones representing a transition between the euryhaline, nearshore environments of *Adetognathus* and the normal-marine, offshore environ-

FIGURE 10.—*Photomicrograph of pellet and lump packstone microfacies, SMF-16/17. Sample GM-1 2.32 m; field of view is 1.0 mm.*

ments dominated by gnathodontid genera such as *Declinognathodus*. Early Carboniferous biofacies that may be comparable to the *Rhachistognathus* biofacies of Davis and Webster (1985) include the *Clydagnathus* and *Mestognathus* biofacies. The *Clydagnathus* biofacies is inferred to have occupied nearshore, high-energy settings transitional between landward, shallow-water, and variable-salinity environments, and more offshore, normal-marine settings (von Bitter and others 1986). The *Mestognathus* biofacies, although typically associated with nearshore, hypersaline tidal-lagoon settings, is also commonly recognized in rocks deposited under shallow-water, high-energy conditions (von Bitter and others 1986). This biofacies may therefore be analogous in part to the *Rhachistognathus* biofacies.

The *Rhachistognathus* biofacies is recognized in all sections of the study. At Granite Mountain, the *Rhachistognathus*-dominated samples correspond with part of the coated and worn bioclast packstone (SMF-10), fine-grained coated bioclast grainstone (SMF-11f), bioclast packstone and grainstone (SMF-12), and lag (SMF-14) microfacies. These microfacies are interpreted to have been deposited near or within the influence of wave or tidal energy on or adjacent to high-energy barrier shoals, or in intermediate zones between restricted nearshore and open offshore environments. As noted by Davis and Webster (1985), even in samples where *Rhachistognathus* reaches its maximum abundance, species of *Adetognathus* or *Declinognathodus* are typically also present. Associated biota in the *Rhachistognathus* biofacies include: (1) locally abundant echinoderms; (2) common bryozoans, brachiopods, calcareous algae, and foraminifers; and (3) rare to locally common ostracodes, mollusks, and trilobites.

CONODONT OCCURRENCES WITHIN INDIVIDUAL MICROFACIES

Plots of average abundance versus Standard Microfacies Type for species of *Adetognathus* and *Rhachistognathus* indicate several interesting trends regarding the distribution of conodonts within specific microfacies. A plot of average species abundance versus SMF Type for *Adetognathus lautus, A. spathus,* and *A. unicornis* (fig. 15) clearly shows the dominance of *A. lautus* in virtually all microfacies in comparison to other *Adetognathus* species. This is especially evident in SMF-12, where the average abundance of *A. lautus* is nearly 10 times that of the other species. The rare conodont elements recovered from SMF-11c and SMF-14 typically consist of large, abraded, and broken platforms. The low abundance of all conodonts in these microfacies is attributed to hydraulic winnowing of any conodont elements originally present, as these are the two most coarse-grained, inferred high-energy microfacies recognized. Conversely, the variable but relatively high conodont abundances in the coated and worn bioclast packstone (SMF-10), fine-grained coated bioclast grainstone (SMF-11f), and ooid grainstone (SMF-15) microfacies could in part be due to localized hydraulic concentration of conodont elements, which may have acted as hydraulic equivalents to the other skeletal grains that constitute these microfacies. The low abundances of *A. spathus* in SMF-15 and of *A. unicornis* in SMF-16/17 may be an artifact of sampling, as these two microfacies are poorly represented in the portions of the measured sections where these conodont species occur.

Somewhat analogous trends are noted for species of *Rhachistognathus* (fig. 16). *Rhachistognathus primus* is the dominant species, showing a maximum abundance within SMF-12. The average abundance of *R. primus* is two to eight times greater than *R. muricatus*, *R. prolixus*, and *R. websteri*. In the event that *R. prolixus* and *R. websteri* represent uncommon morphotypes of *R. primus*, the abundance of *R. primus* over *R. muricatus* within SMF-12 would even be greater. Note also that average abundance of all species of *Rhachistognathus* in most microfacies is generally less than that for *Adetognathus* species in the same microfacies.

Low abundances of gnathodontid conodonts precludes construction of a similar plot for *Gnathodus* species and *Declinognathodus noduliferus*. Based on the sparse occurrence data available, *G. defectus* appears more abun-

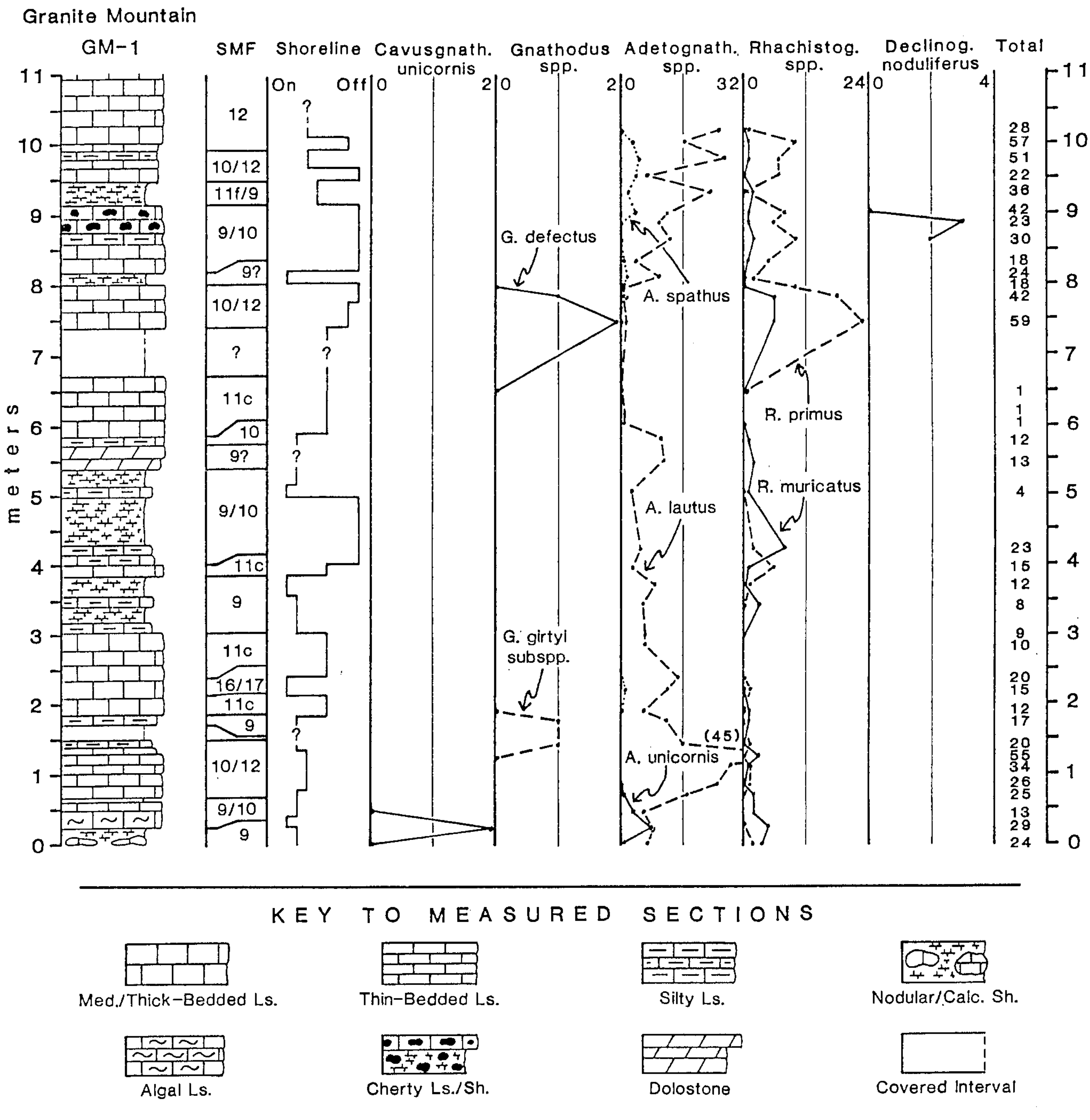

FIGURE 11.—*Ranges and abundances of major conodont species, Granite Mountain section GM-1. All species and total abundance values are Pa elements per kg of sample. SMF column shows Standard Microfacies Types discussed in text. Queried SMF Types are from dolostone or unsampled intervals. Shoreline column shows inferred relative shoreline position, where On and Off correspond to onshore and offshore facies, respectively. Total abundance values are based on all Pa elements recovered, including unidentifiable specimens and rarer species not shown on figure. For complete tabulations of conodont element abundances in all measured sections, see Morrow (1989).*

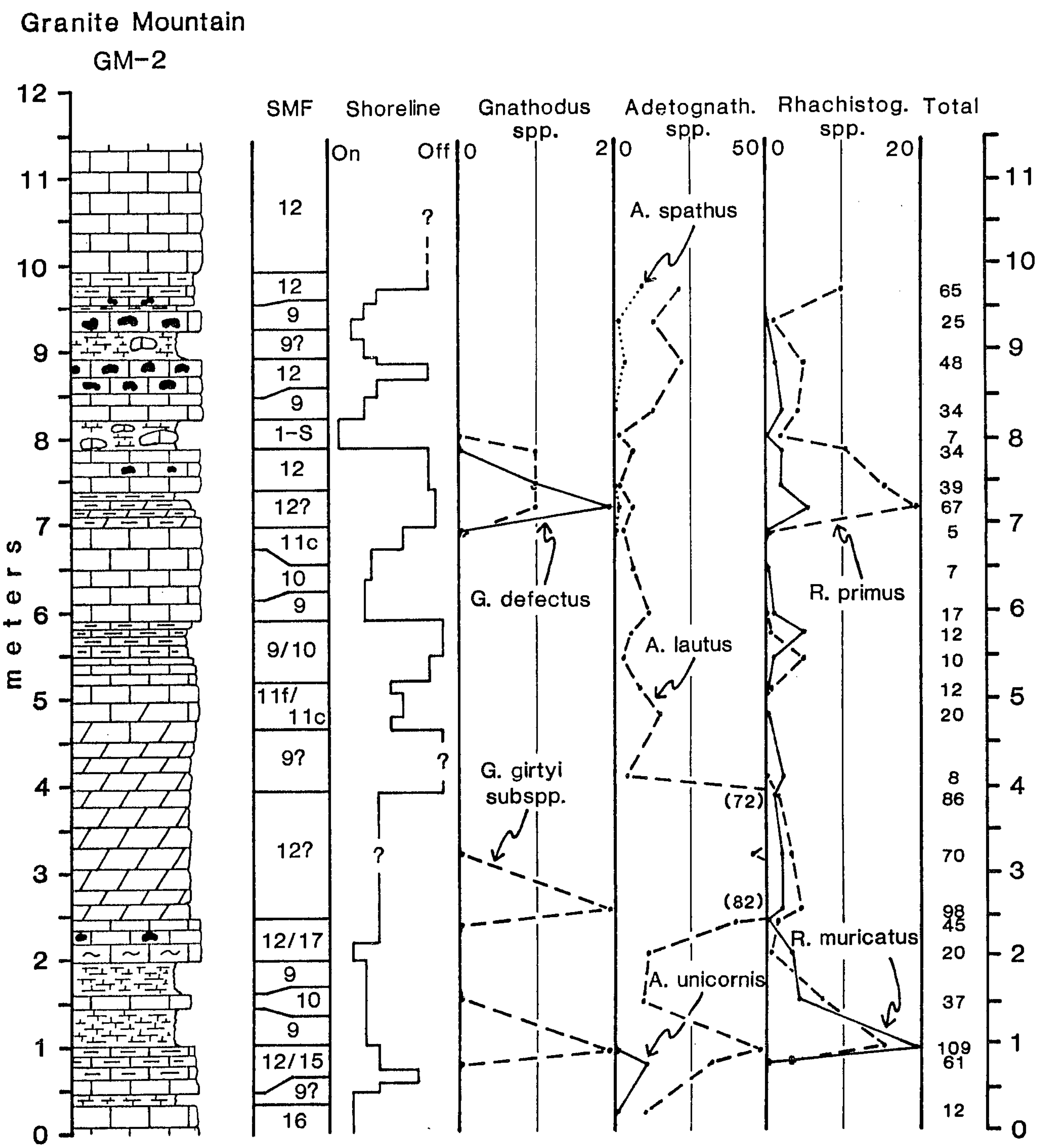

FIGURE 12.—*Ranges and abundance of major conodont species, Granite Mountain section GM-2. See figure 11 for key to lithologic symbols and explanation of columns.*

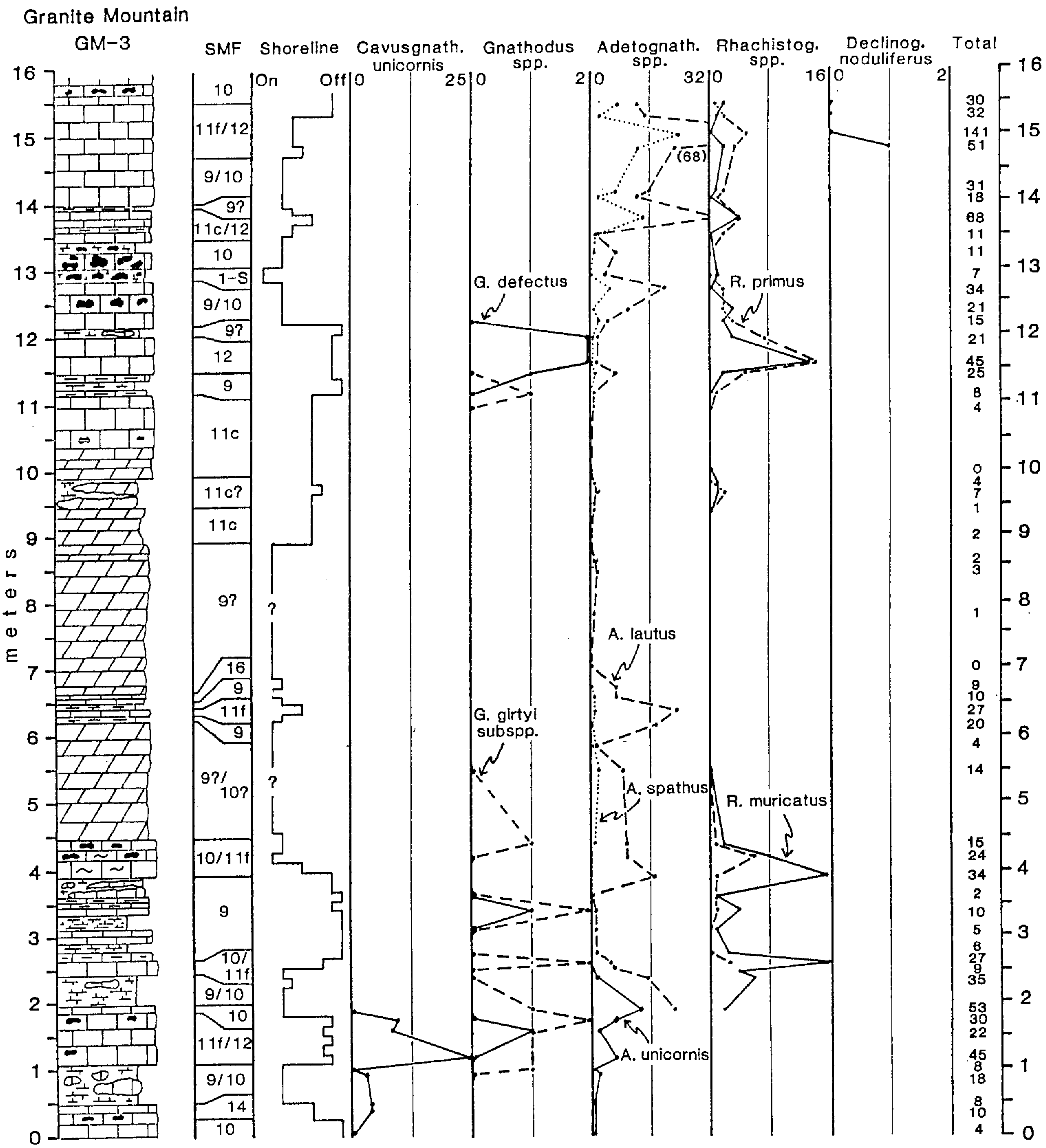

FIGURE 13.—*Ranges and abundance of major conodont species, Granite Mountain section GM-3. See figure 11 for key to lithologic symbols and explanation of columns.*

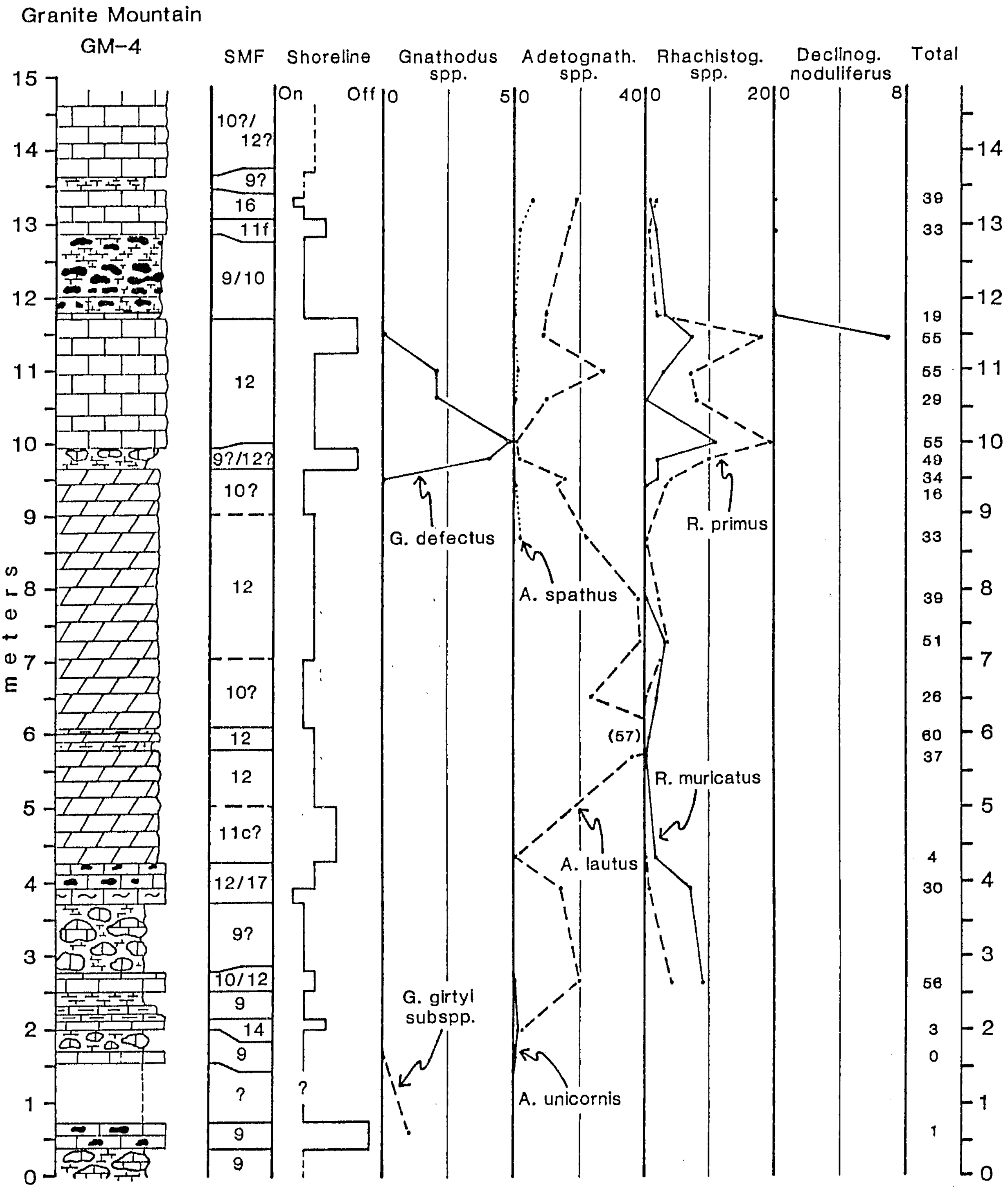

FIGURE 14.—*Ranges and abundance of major conodont species, Granite Mountain section GM-4. See figure 11 for key to lithologic symbols and explanation of columns.*

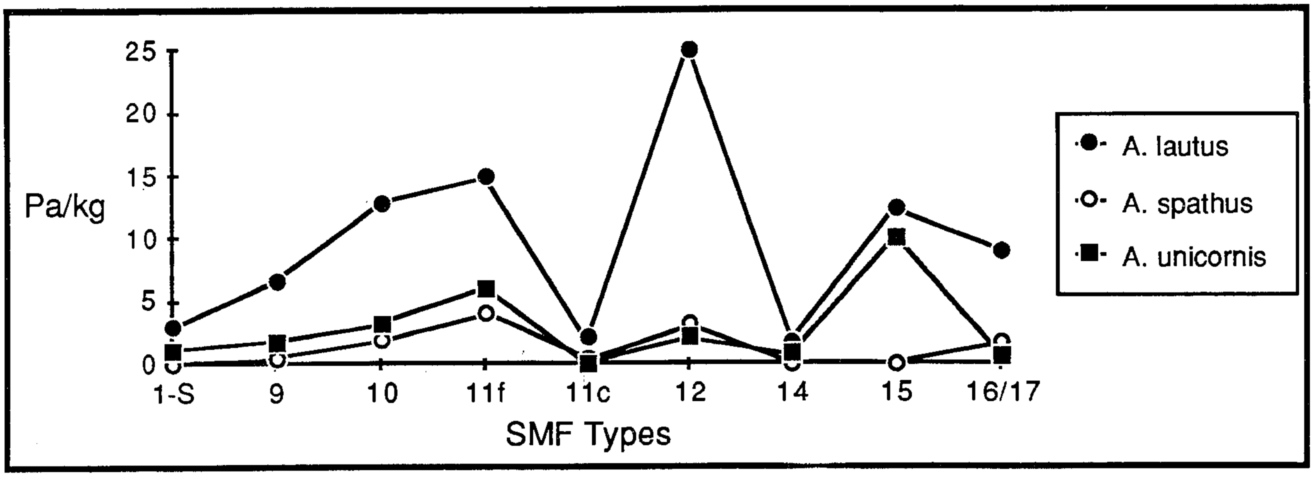

FIGURE 15.—*Plot of* Adetognathus *species abundances versus Standard Microfacies Types (SMF Types), all sections. Conodont abundances, given in Pa elements per kg of sample (Pa/kg), represent average values calculated for all occurrences in the given SMF Type within the range of the given conodont species.*

dant than other *Gnathodus* species, reaching a maximum average value of about 0.75 Pa elements per kg of sample within SMF-12. Typically, *G. defectus* reaches its maximum abundance in samples dominated by *Rhachistognathus*. In addition, several specimens of *G. bilineatus* were recovered from SMF-11c (pl. 3, fig. 10). These conodonts, which are typically altered, fragmented, and abraded, are considered reworked elements. *Declinognathodus noduliferus* appears to reach maximum average abundance within SMF-9 and SMF-12, with values of about 2.5 and 1 Pa elements per kg of sample, respectively.

Based on overall abundances, SMF-12 apparently represents the optimum environmental setting for preservation of conodont elements. This may in part reflect environmental conditions favorable to the living conodont-bearing animal in addition to postmortem conditions favorable for accumulation and preservation of conodont elements. A plot of total *Adetognathus* species versus *Rhachistognathus* species for all SMF-12 samples clearly shows the inverse biofacies occurrence pattern between these two genera within this microfacies (fig. 17). Where *Adetognathus* dominates, *Rhachistognathus* is rare, and vice versa. In approximately 70% of the *Adetognathus*-dominated samples of SMF-12, codiacean and/or dasycladacean green algae forms an abundant to dominant component. In all other aspects, however, the *Adetognathus*-dominated versus *Rhachistognathus*-dominated SMF-12 samples appear identical. This suggests the possibility of further subdividing this microfacies based on

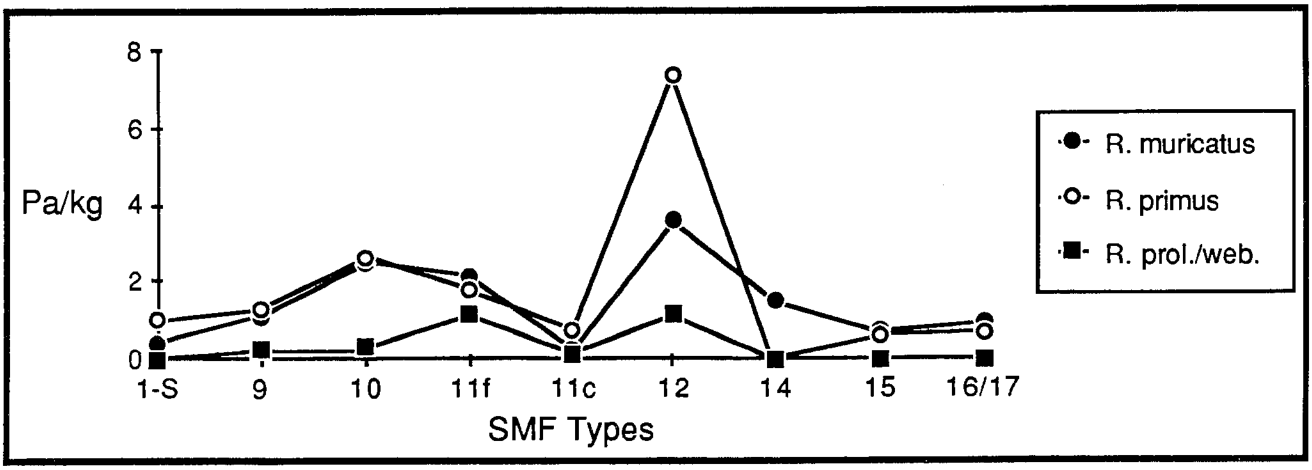

FIGURE 16.—*Plot of* Rhachistognathus *species abundances versus Standard Microfacies Types (SMF Types), all sections. R. prol./web. refers to* R. prolixus *and* R. websteri *abundances combined. See figure 15 for explanation of axes values.*

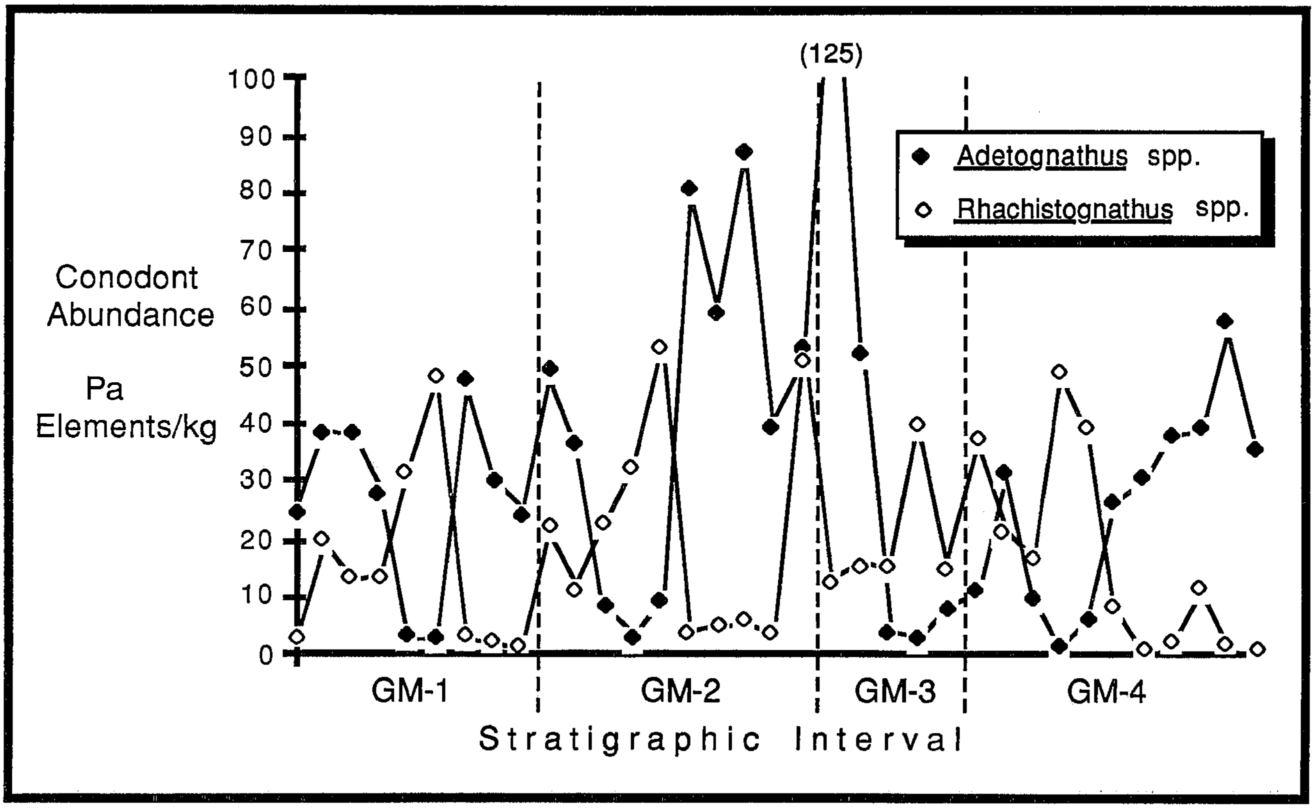

FIGURE 17.—*Plot of total* Adetognathus *and* Rhachistognathus *species abundances within SMF-12, the bioclast packstone and grainstone microfacies, Granite Mountain sections. All abundances are Pa elements per kg of sample. Horizontal axis shows range of measured sections only; no absolute stratigraphic thickness or sample spacing is implied. See figures 11–14 for stratigraphic location of SMF-12 samples.*

the dominant conodont genus present. In several SMF-12 samples from sections GM-2 and GM-4, abundances of *Adetognathus* and *Rhachistognathus* are similar. These mixed biofacies could have formed in transitional zones between the two biofacies settings, or may have resulted from localized postmortem mixing of conodont faunas.

DEPOSITIONAL MODEL

The depositional setting of the lower Ely Limestone at Granite Mountain is considered to have been a relatively high-energy, offshore barrier shoal or bar that separated shallow open-marine facies from a shallow, protected, low-energy, nearshore lagoon environment landward of the barrier shoal (fig. 18). Consistent with the model proposed by Davis and Webster (1985), the high-energy barrier shoal setting is dominated by conodont faunas typical of the *Rhachistognathus* biofacies, whereas the low-energy, nearshore environment is inhabited by conodonts of the *Adetognathus* biofacies. Standard Microfacies Types associated with the barrier shoal setting include SMF-11f, SMF-11c, and SMF-15. These microfacies accumulated at or above wave base, where wave energy winnowed out intergranular lime mud and promoted coating, sorting, and abrasion of allochems, including conodonts.

As noted earlier, SMF-11c is composed of 0.3- to 10-mm-wide grains, with a finer-grained fraction conspicuously lacking. SMF-11f may contain some of the < 0.3 mm fraction that is "missing" from SMF-11c, having formed in a hydraulic regime of slightly lower energy where localized redeposition of suspended finer-grained material from SMF-11c could have occurred. This localized sorting and concentration of finer-grained allochems may be responsible for the variable but relatively high conodont abundances seen in SMF-11f.

The ooid grainstone microfacies (SMF-15) is a rare lithology in the lower Ely Limestone at Granite Mountain. It is tentatively given a separate depositional setting just shoreward of the main barrier shoal, where shallow water and limited circulation promoted the higher temperature and salinity favorable for marine ooid formation (Scoffin 1987). In addition, the lime mud laminations present within SMF-15 may evidence varying deposi-

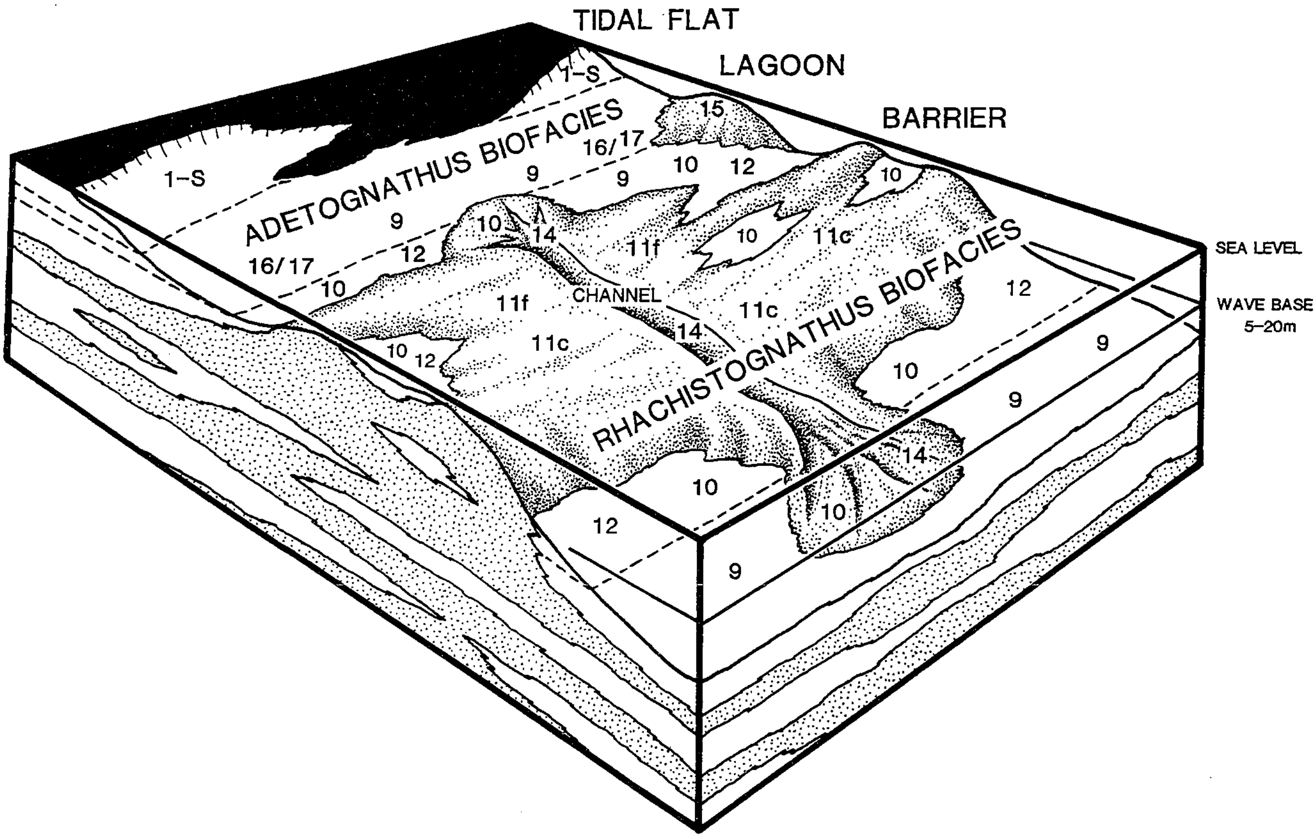

FIGURE 18.—*Proposed depositional model for the lower Ely Limestone, Granite Mountain, showing placement of microfacies and conodont biofacies. Numbers correspond to Standard Microfacies (SMF) Types discussed in text. Stippled pattern represents grainstone facies. Model modified from Inden and Moore (1983), Read (1985), and St. Aubin-Hietpas (1983). Placement of conodont biofacies is after Davis and Webster (1985). Diagram not to scale—great vertical exaggeration.*

tional energy. SMF-11f, SMF-11c, and SMF-15 are typically associated with the unimodal, eastward-dipping, tabular cross-laminations and cross-beds visible in the field. These cross-strata may represent wave-produced flood (shoreward-dipping) accretion beds deposited near the top of the barrier (Davies and others 1971, Inden and Moore 1983).

SMF-14, the lag microfacies, is characterized by variation in both lateral and vertical extent. This microfacies is considered to have accumulated in localized, low-relief tidal channels within the barrier shoal environment. The varied and relatively exotic siltstone and lime mudstone intraclasts present within this microfacies were probably derived from adjacent nearshore or supratidal settings and redeposited within the tidal channel. The coarse grain size of SMF-14 is indicative of generally high-energy conditions that were apparently unfavorable for the accumulation and preservation of conodont elements.

SMF-9, SMF-10, and SMF-12 are thought to have accumulated both shoreward and seaward of the barrier shoal, beyond the direct influence of wave energy. SMF-10, the coated and worn bioclast packstone microfacies, is considered to have formed directly adjacent to grainstone microfacies, where high-energy particles could have been washed into the dominantly lower-energy, lime mud–rich setting of this microfacies. This localized mixing, combined with bioturbation, may be responsible for the large variation in conodont abundances from SMF-10. As previously noted, SMF-12 contains the greatest numbers of conodonts, with calcareous green algae composing an abundant skeletal grain component in samples dominated by *Adetognathus*. Based on alternating dominance of the conodont genera *Adetognathus* and *Rhachistognathus*, SMF-12 is considered to have formed (1) on the onshore side of winnowed shoals, where somewhat restricted conditions allowed dominance of *Adetognathus* species and where shallow, protected conditions also promoted proliferation of calcareous green algae (Ginsburg and others 1971); and (2) on the shallow offshore margins of shoals, transitional to open-marine settings, where adjacent high-energy conditions would have favored species of *Rhachistognathus.*

SMF-1-S and SMF-16/17 are characterized by generally limited faunas occurring with (1) abundant lime mud; (2) common lime mud pellets and lumps; (3) common algal and fenestral fabrics; and (4) common quartz silt and fine quartz sand. These microfacies are interpreted to have formed in protected, nearshore lagoons or coastal ponds with somewhat restricted circulation. Conodont faunas are dominated by species of *Adetognathus.*

The three-dimensional geometry of the winnowed shoal to lagoon environment is considered complex. Modern carbonate barrier shoals and reconstructed ancient examples are typically 2 km or more wide and many km long, forming thin, discontinuous, and elongate bars oriented parallel to shore (Inden and Moore 1983, Read 1985). Often, tidal channels cut across shoals, developing flood and ebb-tide deltas on both onshore and offshore sides (respectively) of the barrier. Vertically stacked sequences of these facies show interfingering of the various wackestone, packstone, and grainstone lithologies, and abrupt lateral changes are common. Subsidence coupled with (1) shifting of environments due to small-scale eustatic changes, (2) variation in carbonate production, or (3) wave and tidal energy fluctuations could be responsible for the interfingering pattern. On the shallow carbonate platform bordering the modern Trucial Coast, wind-driven currents are considered the most important mechanism for sediment movement (Purser and Seibold 1973). Similarly, wind-driven currents and waves from postulated northeast paleo–trade winds (Sandberg and others 1982) may have been important in sediment transport within the lower Ely Limestone.

An analogous barrier-lagoon depositional model was proposed for the Ely Limestone by St. Aubin-Hietpas (1983), who studied the carbonate petrology and paleoecology of Chesterian through Wolfcampian strata in the Burbank Hills and Mountain Home Range of southwestern Millard County, located approximately 100 km to the south of Granite Mountain. Based on this, the Ely Limestone in the Granite Mountain area may have been deposited as part of a much larger barrier-lagoon complex that existed in western Utah during the mid-Carboniferous.

CONCLUSIONS

The nine carbonate microfacies recognized in the study are considered to have been deposited in a shallow-water, nearshore marine setting that was often at or near wave base. These microfacies are dominated by SMF-9 (bioclast wackestone microfacies), SMF-10 (coated and worn bioclast packstone microfacies), and SMF-12 (bioclast packstone and grainstone microfacies), which make up two-thirds to three-fourths of all rocks exposed in the sections. SMF-11 of Wilson (1975) and Flugal (1982) can be further subdivided into two separate microfacies based on the dominate grain-size range within them. Typically, the microfacies present are thin and varied, reflecting a complex interaction of depositional energy, skeletal and/or nonskeletal grain supply, and bioturbation. Diagenetic alteration such as silicification and dolomitization are considered early burial features that altered an essentially normal-marine limestone host. Where conodont type or abundance can be tied to specific limestone microfacies types, it is possible to use conodonts recovered from dolostone intervals to help infer original limestone depositional textures in samples destructively replaced by dolomite.

Conodont faunas are dominated by *Adetognathus* and *Rhachistognathus,* which occur in alternating and recurring peaks that define the *Adetognathus* and *Rhachistognathus* biofacies. Gnathodontid conodont species are rare in all sections and from all microfacies. This scarcity precludes recognition of other previously proposed mid-Carboniferous conodont biofacies based on the dominance of gnathodontid genera. Conodont abundances within specific microfacies reflect both environmental controls acting on the conodont animal and postmortem factors that concentrated or removed conodont elements. *Adetognathus* faunas are dominated by *A. lautus* in all microfacies present. Similarly, *Rhachistognathus primus* appears more common than other *Rhachistognathus* species in most microfacies. Both *Adetognathus* and *Rhachistognathus* reach their maximum abundance within SMF-12, the bioclast packstone and grainstone microfacies. The inverse occurrence pattern of these two genera within this microfacies allows further subdivision of SMF-12, based on the dominant conodont type present.

A high-energy, offshore barrier shoal and protected, nearshore-lagoon depositional setting is inferred for the microfacies of the study. The barrier shoal environment, in which the *Rhachistognathus* biofacies occurs, is dominated by the grainstone microfacies SMF-11f, SMF-11c, and SMF-14. The *Adetognathus* biofacies dominates within the low-energy lagoon setting, which is characterized by the lime mud–rich microfacies SMF-1-S and SMF-16/17. Microfacies present both onshore, offshore, and locally within the barrier shoal include SMF-9, SMF-10, and SMF-12.

ACKNOWLEDGMENTS

Thanks are given to Dr. Robert C. Grayson, Baylor University, and Dr. Charles A. Sandberg, U.S. Geological Survey, who critically reviewed the manuscript. Dr. Larry E. Davis, Washington State University, provided additional constructive suggestions. Their many helpful comments were greatly appreciated. Thanks are also given to the Washington State University Electron Microscopy Center for their assistance in photographing conodont specimens. This project was funded in part by ARCO Oil and Gas Incorporated.

REFERENCES CITED

Austin, R. L., and Davies, R. B., 1984, Problems of recognition and implications of Dinantian conodont biofacies in the British Isles: In Clark, D. L. (ed.), Conodont biofacies and provincialism: Geological Society of America Special Paper 196, p. 195–228.

Baesemann, J. F., and Lane, R. H., 1985, Taxonomy and evolution of the genus *Rhachistognathus* Dunn (Conodonta: Late Mississippian to early Middle Pennsylvanian): Courier Forschungsinstitut Seckenberg, v. 74, p. 93–136.

Barnes, C. R., Rexroad, C., and Miller, J., 1973, Lower Paleozoic provincialism: In Rhodes, F. H. T. (ed.), Conodont paleoecology: Geological Society of America Special Paper 141, p. 157–90.

Collinson, C., 1963, Collection and preparation of conodonts through mass production techniques: Illinois State Geological Survey Circular 343, 16p.

Davies, D. K., Ethridge, F. G., and Berg, R. R., 1971, Recognition of barrier environments: American Association of Petroleum Geologists Bulletin, v. 55, no. 4, p. 550–65.

Davis, L. E., and Webster, G. D., 1985, Late Mississippian to Early Pennsylvanian conodont biofacies in central Montana: Lethaia, v. 18, p. 67–72.

Driese, S. G., Carr, T. R., and Clark, D. L., 1984, Quantitative analysis of Pennsylvanian shallow-water conodont biofacies, Utah and Colorado: In Clark, D. L. (ed.), Conodont biofacies and provincialism: Geological Society of America Special Paper 196, p. 233–50.

Druce, E. C., 1973, Upper Paleozoic and Triassic conodont distribution and recognition of biofacies: In Rhodes, F. H. T. (ed.), Conodont paleozoology: Geological Society of America Special Paper 141, p. 191–237.

Dunn, D. L., 1966, New Pennsylvanian platform conodonts from southwestern United States: Journal of Paleontology, v. 40, p. 1294–1303.

———, 1970a, Conodont zonation near the Mississippian-Pennsylvanian boundary in western United States: Geological Society of America Bulletin, v. 81, p. 2959–74.

———, 1970b, Middle Carboniferous conodonts from western United States and phylogeny of the platform group: Journal of Paleontology, v. 44, p. 312–42.

Epstein, A. G., Epstein, J. B., and Harris, L. D., 1977, Conodont color alteration—an index to organic metamorphism: U.S. Geological Survey Professional Paper 995, 27p.

Flügel, E., 1982, Microfacies analysis of limestones: Springer-Verlag, New York, 633p.

Ginsburg, R., Rezak, R., and Wray, J. L., 1971, Geology of calcareous algae, notes for a short course: Sedimenta I: The Comparative Sedimentology Laboratory, University of Miami, Florida, 63p.

Gordon, M., Jr., Henry, T. W., and Mamet, B. L., 1984, Stop 3—Granite Mountain section: In Lintz, J., Jr. (ed.), Western geological excursions, v. 1: Geological Society of America and Affiliated Societies, Reno, 1984, Field Trip Guidebook, p. 26–38.

———, 1985, Carboniferous succession and Mississippian-Pennsylvanian boundary, Granite Mountain, Utah, U.S.A.: Compte Rendu, 10e Congres International de Stratigraphie et de Geologie du Carbonifere, Madrid, 1983, v. 4, p. 441–50.

Gordon, M., Jr., Henry, T. W., and Sutherland, P. K., 1982, Brachiopod zones delimiting the Mississippian-Pennsylvanian boundary in the United States: In Ramsbottom, W. H. C., Saunders, W. B., and Owen, B. (eds.), Biostratigraphic data for a mid-Carboniferous boundary: International Union of Geological Sciences, Subcommission on Carboniferous Stratigraphy (Symposium), Leeds, 1981, p. 69–76.

Hose, R. K., 1974, Geologic map of the Granite Mountain SW Quadrangle, Juab and Millard Counties, Utah: U.S. Geological Survey Miscellaneous Geologic Investigations Map I-831.

———, 1977, Structural geology of the Confusion Range, west central Utah: U.S. Geological Survey Professional Paper 971, 9p.

Hose, R. K., and Repenning, C. A., 1959, Stratigraphy of Pennsylvanian, Permian, and Lower Triassic rocks of the Confusion Range, west central Utah: American Association of Petroleum Geologists Bulletin, v. 43, no. 9, p. 2167–96.

Inden, R. F., and Moore, C. H., 1983, Chapter 5, Beach: In Scholle, P. A., Bebout, D. G., and Moore, C. H. (eds.), Carbonate depositional environments: American Association of Petroleum Geologists Memoir 33, p. 211–67.

Krukowski, S. T., 1988, Sodium polytungstate: A new heavy-mineral separation medium for the extraction of conodonts from insoluble residues: Journal of Paleontology, v. 62, p. 314–16.

Lane, H. R., and Manger, W. L., 1985, Toward a boundary in the middle of the Carboniferous (1975–1985): Ten years of progress: Courier Forschungsinstitut Seckenberg, v. 74, p. 15–34.

Mamet, B. L., 1982, A report on algal microfacies at the Mississippian-Pennsylvanian boundary in the United States: In Ramsbottom, W. H. C., Saunders, W. B., and Owen, B. (eds.), Biostratigraphic data for a mid-Carboniferous boundary: International Union of Geological Sciences, Subcommission on Carboniferous Stratigraphy (Symposium), Leeds, 1981, p. 52–60.

———, 1984, Algal and foraminiferal biotas and microfacies, Mississippian-Pennsylvanian boundary, Granite Mountain section: In Lintz, J., Jr. (ed.), Western geological excursions, v. 1: Geological Society of America and Affiliated Societies, Reno, 1984, Field Trip Guidebook, p. 84–86.

Merrill, G. K., 1973, Pennsylvanian conodont paleoecology: In Rhodes, F. H. T. (ed.), Conodont paleozoology: Geological Society of America Special Paper 141, p. 239–74.

———, 1987, Cryogenic density separation of conodonts: In Austin, R. L. (ed.), Conodonts: investigative techniques and applications: Ellis Horwood Ltd., Chichester, United Kingdom, p. 63–66.

Merrill, G. K., and Martin, M. D., 1976, Environmental control of conodont distribution in the Bond and Mattoon Formations (Pennsylvanian, Missourian), northern Illinois: In Barnes, C. R. (ed.), Conodont paleoecology: Geological Association of Canada Special Paper 15, p. 243–71.

Merrill, G. K., and von Bitter, P. H., 1976, Revision of conodont biofacies nomenclature and interpretations of environmental controls in Pennsylvanian rocks of eastern and central North America: Royal Ontario Museum Life Sciences Contributions 108, 46p.

———, 1984, Facies and frequencies among Pennsylvanian conodonts: Apparatuses and abundances: In Clark, D. L. (ed.), Conodont biofacies and provincialism: Geological Society of America Special Paper 196, p. 251–61.

Morrow, J. R., 1989, Conodont biostratigraphy, megafossil biostratigraphy, and carbonate petrology, Mississippian-Pennsylvanian boundary strata, Granite Mountain and northern Confusion Range, Juab and Millard Counties, Utah: Master's thesis, Washington State University, Pullman, Washington, 227p.

Morrow, J. R., and Webster, G. D., 1989a, New sedimentologic and paleontologic data on the proposed mid-Carboniferous boundary stratotype, Granite Mountain, west central Utah: Geological Society of America Abstracts with Programs, v. 21, no. 5, p. 119.

———, 1989b, A cryogenic density separation technique for conodont and heavy mineral separations: Journal of Paleontology, v. 63, no. 6, p. 953–55.

———, 1990, New petrographic and faunal data on the proposed Mississippian-Pennsylvanian boundary stratotype, Granite Mountain, west central Utah: Geological Society of America Abstracts with Programs, v. 22, no. 1, p. 29.

Purser, B. H., and Seibold, E., 1973, The principal environmental factors influencing Holocene sedimentation and diagenesis in the Persian Gulf: In Purser, B. H. (ed.), The Persian Gulf, Holocene carbonate sedimentation and diagenesis in a shallow epicontinental sea: Springer-Verlag, New York, p. 1–10.

Rafuse, B. E., 1973, Bathymetry of conodonts from the Bird Spring Formation of Arrow Canyon, Nevada: Master's thesis, Washington State University, Pullman, Washington, 60p.

Read, J. F., 1985, Carbonate platform facies models: American Association of Petroleum Geologists Bulletin, v. 69, no. 1, p. 1–21.

Rich, M., 1977, Pennsylvanian paleogeographic patterns in the western United States: In Stewart, J. H., Stevens, C. H., and Fritsche, E. A. (eds.), Paleozoic paleogeography of the western United States, Pacific Coast Paleogeography Symposium I: Society of Economic Paleontologists and Mineralogists, Pacific Section, Los Angeles, 1977, p. 87–111.

St. Aubin-Hietpas, L. A., 1983, Carbonate petrology of Permo-Carboniferous rocks, southwestern Millard County, Utah: Brigham Young University Geology Studies, v. 30, pt. 1, p. 113–43.

Sandberg, C. A., and Gutschick, R. C., 1984, Distribution, microfauna, and source-rock potential of Mississippian Delle Phosphatic Member of Woodman Formation and equivalents, Utah and adjacent states: In Woodward, J., Meissner, F. F., and Clayton, J. L. (eds.), Hydrocarbon source rocks of Greater Rocky Mountain region: Rocky Mountain Association of Geologists, Denver, p. 135–78.

Sandberg, C. A., Gutschick, R. C., Johnson, J. G., Poole F. G., and Sando, W. J., 1982, Middle Devonian to Late Mississippian geologic history of the Overthrust Belt region, western United States: In Powers, R. B. (ed.), Geologic studies of the Cordilleran thrust belt: Rocky Mountain Association of Geologists, Denver, p. 691–719.

Sandberg, C. A., Poole, F. G., and Gutschick, R. C., 1980, Devonian and Mississippian stratigraphy and conodont zonation of Pilot and Chainman Shales, Confusion Range, Utah: In Fouch, T. D., and Magathan, E. R. (eds.), Paleozoic paleogeography of the west central United States, Rocky Mountain Paleogeography Symposium I: Society of Economic Paleontologists and Mineralogists, Rocky Mountain Section, Denver, 1980, p. 71–79.

Savage, N. M., 1988, The use of sodium polytungstate for conodont separations: Journal of Micropalaeontology, v. 7, no. 1, p. 39–40.

Scoffin, T. P., 1987, An introduction to carbonate sediments and rocks: Chapman and Hall, New York, 274p.

Seddon, G., and Sweet, W. C., 1971, An ecologic model for conodonts: Journal of Paleontology, v. 45, p. 869–80.

Steele, G., 1960, Pennsylvanian-Permian stratigraphy of east central Nevada and adjacent Utah: In Guidebook to the geology of east central Nevada: Intermountain Association of Petroleum Geologists and Eastern Nevada Geological Society, p. 91–113.

Stevens, C. H., and Armin, R. A., 1983, Microfacies of the Middle Pennsylvanian part of the Oquirrh Group, central Utah: Geological Society of America Memoir 157, p. 83–100.

Tynan, M. C., 1980, Conodont biostratigraphy of the Mississippian Chainman Formation, western Millard County, Utah: Journal of Paleontology, v. 54, p. 1282–1309.

von Bitter, P. H., 1972, Environmental control of conodont distribution in the Shawnee Group (Upper Pennsylvanian) of eastern Kansas: The University of Kansas Paleontological Contributions, Article 59, p. 1–105.

von Bitter, P. H., Sandberg, C. A., and Orchard, M. J., 1986, Phylogeny, speciation, and palaeoecology of the Early Carboniferous (Mississippian) conodont genus *Mestognathus:* Royal Ontario Museum Life Sciences Contributions 143, 115p.

Wardlaw, B. R., 1984, Conodont faunas, Mississippian-Pennsylvanian boundary, Granite Mountain section: In Lintz, J., Jr. (ed.), Western geological excursions, v. 1: Geological Society of America and Affiliated Societies, Reno, 1984, Field Trip Guidebook, p. 82–84.

Webster, G. D., 1969, Chester through Derry conodonts and stratigraphy of northern Clark and southern Lincoln Counties, Nevada: University of California Publications in Geological Sciences, v. 79, 121p.

———, 1984, Conodont zonations near the Mississippian-Pennsylvanian boundary in the eastern Great Basin: In Lintz, J., Jr. (ed.), Western geological excursions, v. 1: Geological Society of America and Affiliated Societies, Reno, 1984, Field Trip Guidebook, p. 78–82.

Webster, G. D., Gordon, M., Jr., Langenheim, R. L., and Henry, T. W., 1984, The Mississippian-Pennsylvanian Boundary in the eastern Great Basin (Field Trip 1): In Lintz, J., Jr. (ed.), Western geological excursions, v. 1: Geological Society of America and Affiliated Societies, Reno, 1984, Field Trip Guidebook, p. 1–86.

Welsh, J. E., and Bissell, H. J., 1979, The Mississippian and Pennsylvanian (Carboniferous) Systems in the United States—Utah: In The Mississippian and Pennsylvanian (Carboniferous) Systems in the United States: U.S. Geological Survey Professional Paper 1110-M-DD, p. Y1–Y35.

Wilson, J. L., 1975, Carbonate facies in geologic history: Springer-Verlag, New York, 471p.